(12) INTERNATIONAL APPLICATION PUBLISHED UNDER THE PATENT COOPERATION TREATY (PCT)

(19) World Intellectual Property Organization
International Bureau

(43) International Publication Date
04 October 2018 (04.10.2018)

WIPO | PCT

(10) International Publication Number
WO 2018/182432 A1

(51) International Patent Classification:
H02J 50/00 (2016.01) *H04B 5/00* (2006.01)
H02M 5/04 (2006.01)

(21) International Application Number:
PCT/NZ2018/050039

(22) International Filing Date:
28 March 2018 (28.03.2018)

(25) Filing Language: English

(26) Publication Language: English

(30) Priority Data:
730582 28 March 2017 (28.03.2017) NZ

(71) Applicant: **AUCKLAND UNISERVICES LIMITED** [NZ/NZ]; Level 10, 70 Symonds Street, Auckland 1010 (NZ).

(72) Inventors; and

(71) Applicants: **THRIMAWITHANA, Duleepa Jayanath** [NZ/NZ]; 2/241 Marua Road, Mt Wellington, Auckland 1051 (NZ). **MADAWALA, Udaya Kumara** [NZ/NZ]; 10 Kauriki Terrace, Stonefields, Auckland 1072 (NZ). **KALRA, Gaurav Rajesh** [NZ/NZ]; 34 Oakdale Rd, Mt.Roskill, Auckland 1041 (NZ). **RIAR, Baljit Singh** [NZ/NZ]; 1-831A Manukau Road, Royal Oak, Auckland 1023 (NZ). **NEUBURGER, Martin** [DE/DE]; Hochschule Esslingen, Fakultat Mechatronik und Elektrotechnik, Standort Goppingen, Robert-Bosch-Str. 1, 73037 Göppingen (DE). **RUDDELL, Steven Ian** [NZ/NZ]; 9B / 6 Whitaker Place, Grafton, Auckland 1010 (NZ). **ZANE, Regan Andrew** [US/US]; 124 Mountain View Drive, Hyde Park, Utah 84318 (US).

(74) Agent: **BALDWINS INTELLECTUAL PROPERTY**; Level 15, HSBC House, 1 Queen Street, Auckland 1010 (NZ).

(81) Designated States *(unless otherwise indicated, for every kind of national protection available)*: AE, AG, AL, AM, AO, AT, AU, AZ, BA, BB, BG, BH, BN, BR, BW, BY, BZ, CA, CH, CL, CN, CO, CR, CU, CZ, DE, DJ, DK, DM, DO, DZ, EC, EE, EG, ES, FI, GB, GD, GE, GH, GM, GT, HN, HR, HU, ID, IL, IN, IR, IS, JO, JP, KE, KG, KH, KN, KP, KR, KW, KZ, LA, LC, LK, LR, LS, LU, LY, MA, MD, ME, MG, MK, MN, MW, MX, MY, MZ, NA, NG, NI, NO, NZ, OM, PA, PE, PG, PH, PL, PT, QA, RO, RS, RU, RW, SA, SC, SD, SE, SG, SK, SL, SM, ST, SV, SY, TH, TJ, TM, TN, TR, TT, TZ, UA, UG, US, UZ, VC, VN, ZA, ZM, ZW.

(84) Designated States *(unless otherwise indicated, for every kind of regional protection available)*: ARIPO (BW, GH, GM, KE, LR, LS, MW, MZ, NA, RW, SD, SL, ST, SZ, TZ, UG, ZM, ZW), Eurasian (AM, AZ, BY, KG, KZ, RU, TJ, TM), European (AL, AT, BE, BG, CH, CY, CZ, DE, DK,

(54) Title: AC-AC CONVERTER

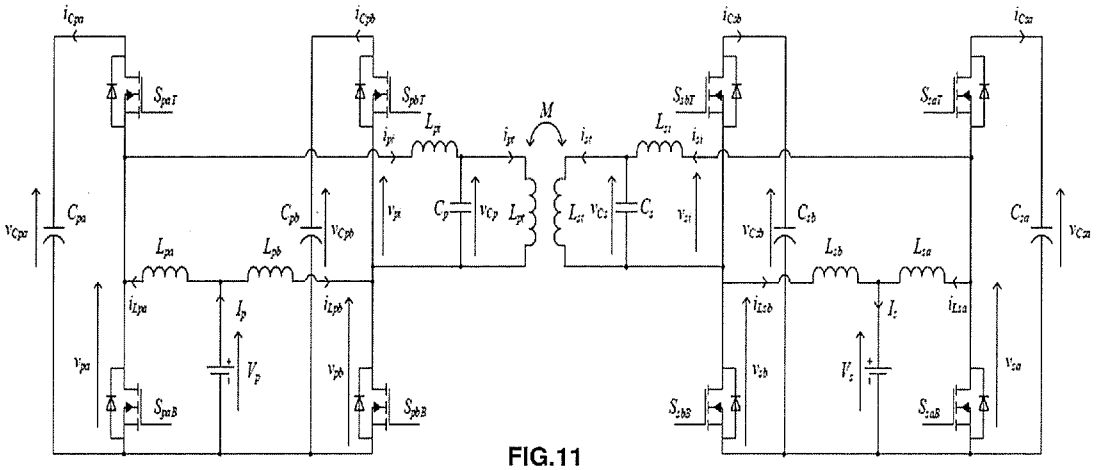


FIG.11

(57) Abstract: The present invention relates to a AC-AC converter, which has particular relevance to a converter for an inductive or capacitive (wireless) power transfer system. More specifically, the current invention discloses an AC-AC converter comprising a bridge circuit having a first leg and a second leg, each leg including a high switch and a low switch, the high switches being connected to a first energy source and the low switches being connected to ground, a coupling network(s) having a first connection between the switches of the first leg and a second connection between the switches of the second leg, a second (or multiple secondary) energy source(s) connected between the coupling network(s) and ground.

WO 2018/182432 A1

[Continued on next page]

EE, ES, FI, FR, GB, GR, HR, HU, IE, IS, IT, LT, LU, LV, MC, MK, MT, NL, NO, PL, PT, RO, RS, SE, SI, SK, SM, TR), OAPI (BF, BJ, CF, CG, CI, CM, GA, GN, GQ, GW, KM, ML, MR, NE, SN, TD, TG).

Published:

— *with international search report (Art. 21(3))*
— *before the expiration of the time limit for amending the claims and to be republished in the event of receipt of amendments (Rule 48.2(h))*
— *in black and white; the international application as filed contained color or greyscale and is available for download from PATENTSCOPE*

AC-AC CONVERTER

Field of the Invention

The present invention relates to an AC-AC converter, which has particular relevance to a converter for an inductive or capacitive (wireless) power transfer system.

In particular, though not solely, the present invention aims at providing an improved circuit topology that enables the use of DC switches to generate an AC output from an AC input source. Additionally, this approach also lowers the required capacitance for a given output power ripple, thus further reducing cost, and improving energy density and reliability. It also provides a voltage boosting feature, which is lacking in existing direct AC-AC converters.

Background

As the uptake of battery powered devices continues to grow around the world, effective charging techniques, which are safe, reliable and convenient, have become a major point of discussion. Traditionally, conductive charging techniques (hard-wired chargers, where a physical connection between a battery and an external energy source, most likely the utility grid) have been used, however these techniques are inconvenient for users, and often raise concerns over user safety and reliability, especially at higher power levels and during harsh weather conditions. Consequently, there has been a shift towards wireless chargers, which are inherently safer, more convenient and lack any physical contacts. Inductive Power Transfer (IPT), which has been used in a wide variety of applications, including powering automated guided vehicles (AGV); materials handling; charging of portable electronic devices and powering biomedical devices and Electric Vehicle (EV) charging, is currently the preferred technology for implementing wireless chargers. This preference is mainly due to the high galvanic isolation and flexibility offered by IPT based wireless chargers while still being able to achieve efficiencies comparable to wired chargers.

The current uptake in IPT charging is highlighted by the introduction of specifications, standards and guidelines for IPT based chargers, which intends to ensure interoperability between various systems. For example, portable communication or computing devices may require multiple different plug arrangement. Another example of particular relevance is electric vehicle (EV) charging in which wire charging techniques suffer from reliability and safety issues at high power levels. To minimise safety concerns for EV's, minimal user input is preferred to initiate the charging process therefore there has been a shift towards wireless charging techniques. Standards such as SAE J 2954, provides specification guidelines on

the implementation of wireless chargers for EV's. SAE J2954 specifies wireless charging through inductive power transfer (IPT), which is currently the preferred technology for wireless power applications.

IPT systems are capable of transferring very high levels of power through a safe and reliable inductive link. This has led to numerous industrial applications in the past 20 years including factory automation, clean room applications and monorail systems. Furthermore, the inherent safety provided by this technology has also led to many biomedical applications, see for example, G. A. Covic and J. T. Boys, "Modern Trends in Inductive Power Transfer for Transportation Applications," IEEE Journal of Emerging and Selected Topics in Power Electronics, vol. 1, pp. 28-41, 2013.

The majority of IPT based EV chargers reported to date only allow unidirectional power flow, typically from the utility grid to the EV battery. However, the recent introduction of bidirectional IPT (BD-IPT) technologies not only improves system efficiency and flexibility, but also enables Vehicle to Grid/Grid to Vehicle (V2G/G2V) services. These services, which are expected to become an integral part of future EV charging infrastructure, include the absorption of power variances produced by renewable energy sources, reactive power injection for grid voltage regulation and harmonics absorption for improved power quality. Overall, such services can further enhance the use of renewable energy sources, while also providing an additional revenue stream for EV owners.

Wide-bandgap devices, such as silicon-carbide or gallium-nitride devices, provide the possibility to operate IPT systems at higher frequencies and higher voltages. Furthermore, wide bandgap devices have much lower on state resistances and negligible reverse recovery losses when compared to silicon devices. Thus, IPT systems can benefit from improved power density and efficiency with these devices. More specifically, operating at higher voltages will allow for lowered current in magnetic couplers, hence reducing resistive losses and unwanted heating effects. A higher driving voltage also opens up opportunities to drive multiple series connected couplers or even elongated tracks, which will be beneficial in high power applications such as fast charging and in-motion charging. Existing IPT systems, which utilise conventional switch-mode power converters, lack the capability to utilise wide bandgap devices to their full voltage rating.

This limitation can be mainly attributed to limited supply and output voltages found in typical applications. Increasing the operating voltage of these systems can be a simple, yet expensive solution. For example, additional power converters can be used to boost/buck

supply/load voltages, however an increased component count and reduced efficiency lead to an undesired solution.

Objects of the Invention

It is an object of the invention to provide a converter which will at least go some way to overcoming disadvantages of existing systems, or which will at least provide a useful alternative to existing systems.

Further objects of the invention will become apparent from the following description.

Summary of Invention

Accordingly in one aspect the invention is said to consist in
a boost active bridge converter comprising:
a bridge circuit having a first leg and a second leg, each leg including a high switch and a low switch, the high switches being connected to a first energy source and the low switches being connected to ground,
a coupling network(s) having a first connection between the switches of the first leg and a second connection between the switches of the second leg,
a second (or multiple secondary) energy source(s) connected between the coupling network(s) and ground.

In another aspect the invention consists in a
a AC-AC converter comprising:
a bridge circuit having a first leg and a second leg, each leg including a high switch and a low switch, the high switches being connected to a first energy source and the low switches being connected to ground,
a coupling network(s) having a first connection between the switches of the first leg and a second connection between the switches of the second leg,
a second (or multiple secondary) energy source(s) connected between the coupling network(s) and ground.

The first energy source may comprise a capacitor. A separate energy source, for example a capacitor may be provided connected between each high switch and ground.

A third energy source may be connected in parallel with the coupling network (directly or through a another coupling network). The third energy source may comprise an AC energy source.

The coupling network comprises one or more inductors (or capacitors) arranged to interface the second (or third) energy source effectively with the first and second legs.

The coupling network may comprise a first inductive element connected between the second energy source and the switches of the first leg, and a second inductive element connected between the second energy source and the switches of the second leg. The first and second inductive elements may be coupled. A third inductive element may be connected between the first and second inductive elements and the second energy source.

A controller is provided to control the switches of the boost active bridge. The controller is also configured to control the duty cycle and/or phase of the switches.
The controller may have one or more input control variables as inputs for controlling the switches. Control of the duty cycle of the switches can control two output variables of the converter. The two output parameters can comprise the voltage of each first energy source and the magnitude of the fundamental voltage across the third energy source.

Alternatively, the controller may control the energy transfer between each source to optimise the operation (efficiency and power transfer) of the converter.

The controller may control the duty cycle of the legs symmetrically.

In another aspect the invention may broadly be said to consist in a dual bridge converter comprising two converters according to the preceding statement wherein the AC energy sources are coupled to each other.

In one example the coupled AC energy sources provide isolation.

In one example the AC sources are loosely coupled. The loose coupling allows inductive power transfer between the converters.

In another aspect the invention broadly provides an IPT converter comprising:
a bridge circuit having a first leg and a second leg, each leg including a high switch and a low switch, the high switches being connected to a first energy source and the low switches being connected to ground,
a coupling network(s) having a first connection between the switches of the first leg and a second connection between the switches of the second leg,

a second energy source connected between the coupling network and ground (directly or through a another coupling network), and
a magnetic coupler connected in parallel with the coupling network(s).

The first energy source may comprise a capacitor. A separate energy source, for example, a capacitor may be provided connected between each high switch and ground.

The magnetic coupler includes a coil which may be series or parallel tuned. The magnetic coupler may comprise a primary apparatus or a secondary (pick-up) apparatus, or may be configured for bi-directional power transfer.

In another aspect the invention broadly provides an IPT system comprising at least one converter according to the preceding statement.

In another aspect the invention broadly provides a method of controlling a boost active bridge converter, the method comprising the steps of:
controlling the bridge switches to alternately apply current from a first energy source to a coupling network which couples the converter to a second energy source, and
controlling the duty cycle of the or selected bridge switches to control the voltage across a third energy source connected in parallel with the coupling network.

The energy flow between first, second and third energy sources can be bi-directional.

The concept can be extended with multiple legs, for example to supply a three-phase system.

In another aspect the invention broadly provides a converter comprising:
an H bridge having a DC side and an AC side,
a first energy source connected to the DC side,
a coupling network connected to the AC side, and
a second energy source connected to the coupling network.

In one example the coupled AC energy sources provide isolation.

In one example the AC sources are loosely coupled. The loose coupling allows inductive power transfer between the converters.

Additionally, if the secondary converter is capable of bidirectional power flow, the grid current can also be controlled to deliver power to the grid.

In another aspect the invention broadly provides an IPT system (50) comprising at least one converter according to the preceding statement.

This functionality enables Vehicle to Grid (V2G) services such as, voltage/frequency regulation, and reactive power/harmonics compensation.

As used herein the term `and/or_ means `and_ or `or_ or both.

As used herein `(s)_ following a noun means the plural and/or singular forms of the noun.

The term `comprising_ as used in this specification means `consisting at least in part of_. When interpreting statements in this specification which include that term, the features, prefaced by that term in each statement, all need to be present, but other features can also be present. Related terms such as `comprise_ and `comprised_ are to be interpreted in the same manner.

It is intended that reference to a range of numbers disclosed herein (for example, 1 to 10) also incorporates reference to all rational numbers within that range (for example, 1, 1.1, 2, 3, 3.9, 4, 5, 6, 6.5, 7, 8, 9 and 10) and also any range of rational numbers within that range (for example, 2 to 8, 1.5 to 5.5 and 3.1 to 4.7).

The entire disclosures of all applications, patents and publications, cited above and below, if any, are hereby incorporated by reference.

The disclosed subject matter also provides method or system which may broadly be said to consist in the parts, elements and features referred to or indicated in this specification, individually or collectively, in any or all combinations of two or more of those parts, elements or features. Where specific integers are mentioned in this specification which have known equivalents in the art to which the invention relates, such known equivalents are deemed to be incorporated in the specification.

Other aspects of the invention may become apparent from the following description which is given by way of example only and with reference to the accompanying drawings.

Drawing Description

A number of examples of the invention will now be described by way of example with reference to the drawings as follows.

Figure 1 is a circuit diagram showing the topology of a converter of the present invention, referred to in this document as a boost active bridge (BAB) converter.

Figure 2 is a general circuit diagram showing the integration of two different energy sources.

Figure 3 is a circuit diagram of an IPT technology based EV charger utilising a converter (BAB) of the present invention.

Figure 4 shows examples of different coupling topologies that can be used with a converter of the present invention, for example, (a) decoupled inductors, (b) partially coupled inductors, and (c) tightly coupled inductors.

Figures 5 to 5E show voltage waveforms produced by the converter (BAB) of the present invention.

Figure 6 is a graph showing Efficiency vs. % regulation for both an active bridge primary to a boost active bridge secondary AB-BAB and a traditional dual active bridge (DAB) configurations.

Figure 7 is a circuit diagram of DBAB based grid connected bi-directional (BD)-IPT system for V2G/G2V applications.

Figure 8 shows simulated waveforms produced by a grid connected DBAB, (a) Soft DC-link voltage and boosted converter voltage, (b) Grid input voltage and current, (c) Voltage modulation on secondary DC side capacitors, (d) Output power.

Figure 9 illustrates a dynamic vehicle charging application of a converter (BAB) of the present invention.

Figure 10 illustrates another example of an IPT system incorporating a BAB topology.

Figure 11 illustrates another example of BAB-based BT-IPT system topology.

Figures 12 to 12C are graphs showing voltages produced by the BAB utilising the proposed switching scheme at (a) Dx = 50%, (b) Dx = 60% and (c) Dx = 40%.

Figure 13 illustrates equivalent phasor domain representation of the LCL networks.

Figure 14 depicts an example of graph showing output power normalised to rated output power of the BAB system, as function of Dp and Ds.

Figure 15 shows the ZVS range of the BAB system operating with a switching frequency of 85 kHz, a tuned frequency of 87 kHz and the DC inductors all designed to 430 uH.

Figure 16 shows the ZVS range of the BAB system operating with a switching frequency of 85 kHz, a tuned frequency of 88 kHz and the DC inductors all designed to 170 uH.

Figure 17 depicts another example of graph showing output power normalised to rated output power of the BAB system, as function of Dp and Ds.

Figure 18 shows the graphs of theoretical and experimental waveforms when operating at 50% duty cycle.

Figure 19 shows the graphs of theoretical and experimental waveforms when operating at 60% duty cycle.

Figures 20 to 20C illustrates the graphs of Experimental current waveforms produced by the primary BAB at (a) 60%, (b) 50% and (c) 40% duty-cycles.

Figure 21 illustrates the Efficiency comparison between the BAB based system and a full-bridge based system over varying loads in a graphical form.

Detailed Description of the Drawings

Over the last decade, a number of bi-directional inductive power transfer systems (BD-IPT) that are suitable for wireless grid integration of electric vehicles (EVs) have been developed. These developments have been fuelled by the enhanced efficiency and spatial tolerance offered by BD-IPT systems, while also enabling the provision of Vehicle-to-Grid (V2G) services. A typical BD-IPT system utilises two synchronised full-bridge converters to drive the primary and secondary magnetic couplers, thus enabling bi-directional power transfer. These full-bridge converters are often operated at fixed-duty cycles to minimize switching losses as well as the generation of harmonics. Additional pre/post power regulation stages are therefore employed to cater for a wide range of loading conditions, at the expense of cost and power density. As an alternative solution, the present invention proposes a novel power converter, named a Boost Active Bridge (BAB), to replace the full-bridge converters.

According to an example of the present invention, the BAB topology provides a converter circuit topology and method to integrate or control additional AC/DC energy sources to the AC-side of an active full bridge. This is achieved at least in part by including an inductor

topology which couples additional DC/AC energy sources to the AC side of the active bridge. The inductor topology may comprise uncoupled, partially coupled, or fully coupled inductors, which act to reduce circulating currents and reduce physical size of components.

A split DC-link is used to allow each inverter leg to operate at a slightly different DC voltage, allowing mismatched duty cycles and simplifying control. The split DC-link is provided by using a separate capacitor for each leg of the bridge. The regulation techniques, described below, allow for two power dependent variables to be adjusted with just one control input. This results in more efficient operation when power regulation is required.

The converter and methods herein described can be used in a number of different applications, including but not limited to the following technologies:

- ð Wireless dynamic electric vehicle charging.
- ð Wireless/wired stationary electric vehicle charging.
- ð Grid connected bi-directional inductive power transfer systems used in vehicle to grid (V2G) / grid to vehicle(G2V) applications.
- ð Fuel cell or Photovoltaic isolated grid connection.

The converter of the present invention is referred to in this document as a `Boost Active Bridge_ or BAB converter. It provides an inexpensive solution which is capable of fully utilising the voltage rating of wide bandgap devices, when the supply/output voltage is significantly less than the device ratings. A system diagram of a BAB, which can act as a DC to AC converter with an integrated boost stage, is shown in Fig. 1. As evident from this diagram, a BAB enables the integration of multiple energy sources with different voltage ratings.

Referring to Figure 1, a BAB converter is shown, generally referenced 1. The converter comprises an active bridge in the form of an H-bridge having a first leg a and a second leg b. Each leg has two switches. A high switch S1 on leg a and another high switch S2 on leg b, and a low switch S3 on leg a and another low switch S4 on leg b. The low switches S3 and S4 are connected to ground 5, and the high switches S1 and S2 are connected to a first energy source comprising energy source 4 and/or capacitor Vc. The first energy source is connected between the high switches and ground. As will be described below, this may simply be a capacitor, and may comprise a separate capacitor for each high switch i.e. a separate capacitor in parallel with each leg. It should be noted that, although the example shown in Figure 1 shows a converter with 2 legs, the concept discussed can be applied to a converter with multiple legs, for example a three-phase converter.

A coupling network 6 has a first connection 7 between the switches S1 and S3 of the first leg and a second connection 8 between the switches S2 and S4 of the second leg. A second energy source 9 is connected to the coupling network, being between the coupling network 6 and ground 5.

A third energy source 10, being an AC energy source, is connected to connection points 7 and 8 i.e. in parallel with the coupling network 6.

A controller 15 comprising a control circuit receives one or more input control variables 16 and has outputs 17 to control switches S1-S4 to achieve control of one or more output variables of the converter, for example control of Vout or Iout. Controller 15 switches S1 and S3 in a complementry fashion, therefore for example when S1 is ON, then S2 OFF. Swithes S2 and S4 are also operated similarly in a complementry fashion. The ON time of S1 and S3 are controlled together with the time-shift (phase-shift) between the control signals applied to each leg to regulate the power flow between each source. As an example when switches S1 and S4 are ON then switches S2 and S3 are OFF so that the voltages at points 7 and 8 are out of phase. For convenience this is referred to in the following description as driving the legs a and b out of phase with each other.

Another way of describing the BAB 1 arrangement is a first energy source connected to the DC side of the H-bridge and a second energy source in parallel with a coupling network connected to the AC side of the H-bridge.

The operation of a BAB is discussed below with reference to its applications in IPT systems. However it should be noted that the proposed topology is not limited to this application and can be applied in conventional power converters. Figure 2 illustrates a general application of the proposed technology. Referring to Figure 2, one or more BAB converters are used to facilitate the integration of multiple energy sources through an isolation technology 20, such inductive power transfer (IPT), capacitive power transfer (CPT) a transformer. The BAB can be used as the primary converter 11, secondary converter 12 or as both. The isolation technology 20 effectively couples the AC energy source 10 from a BAB converter to the AC side of a conventional converter or another BAB converter. Utilising the BAB as both the primary and secondary converter enables bi-directional power flow in which case the isolation technology 20 effectively couples the BAB converters so that each converter comprises the energy source 10 of the other AC energy sources 10 of each BAB converter. A bi-directional configuration can be known as a dual BAB or a DBAB. A BAB in

primary/secondary together with a traditional active bridge (AB) in the secondary/primary can also be used to transfer bi-directional power in some applications. The energy sources 13 and 14 may include, but are not limited to, renewable energy sources, battery storage, fuel cell, utility grid etc. Isolation technologies may include, but are not limited to inductive power transfer, capacitive power transfer, high and low frequency transformers etc. For the BAB converters used in the arrangement shown in Figure 2, the energy sources 13 and/or 14 will comprise the energy source 9 shown in Figure 1.

Some more specific examples of the proposed BAB converter topology will now be described below.

Example #1: IPT Technology based EV charger

The following example applies the BAB in an IPT technology based EV charger, nonetheless the operating principles discussed are relevant for any of the aforementioned applications.

This example is shown in Fig. 3, where an IPT primary circuit is shown generally referenced 30 which energises a primary magnetic coupler Lp to supply power inductively to a secondary circuit 31 which includes a BAB converter 1. The BAB simultaneously boosts the EV battery B1 voltage, and applies a high frequency voltage across the secondary magnetic coupler Ls. To achieve this, both inverter legs a and b are operated nominally at 50% duty cycle and 180 degrees out of phase with each other. In a practical system it is improbable that both inverter legs operate at an identical duty cycle, hence resulting in circulating DC current through the coupling topology. To counteract this, the DC side capacitor is split into two independent capacitors Ca and Cb, one for each inverter leg a ,b. This will provide an energy source that allows each inverter leg to operate at a slightly different DC voltage, thus ensuring that the average value of V_{sa} and V_{sb} are equal.

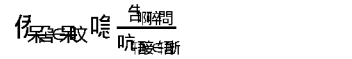
There are three different coupling topologies that can be used to provide the coupling network 6. The coupling network 6 connects the EV battery (B_1) to the BAB, as shown in Fig. 4. Topology 4(a) consists of two decoupled inductors L1 and L2, however a coupled inductor, or coupled inductors, is advantageous as it can reduce the current ripple or reduce the amount of inductance required.

Topology 4(b) consists of a loosely coupled inductor L1/L2, this allows for energy to be stored in the leakage inductance.

Contrastingly, topology 4(c) consists of a tightly coupled inductor L1/L2, here an external inductor L3 is required for energy storage.

Since the two nodes 7 and 8 connecting the coupling network 6 to the BAB are driven 180 degrees out of phase, the current ripple through each node is also 180 degrees out of phase.

This results in almost zero current ripple seen by B_1. B_1 and C_a are connected through the coupling network and one inverter leg (54, referred to for convenience as 5a), this can also be seen as an interconnection through a boost converter. Similarly, B_1 is connected to C_b through the coupling network.



(1)



(2)

Equation 1, where $D_{sa/sb}$ represents the duty cycle of inverter leg `a_ and leg `b_ respectively, can be used to determine the voltage ratio between the EV battery voltage (V_{out}) and $V_{ca/cb.}$ 5b in Figure 3 is represented by 53. Clearly, a nominal duty cycle of 50% results in double the EV battery voltage applied across each inverter leg capacitor. Moreover, this results in double the voltage across the secondary compensation network shown in Fig. 2. Assuming an active bridge is the primary converter in Fig. 2, the power transfer can be calculated using Equation 2. In a series-series IPT system (i.e. the magnetic couplers are series compensated such that Cp is in series with Lp and Cs is in series with Ls), such as this example, the output power is inversely proportional to mutual inductance in between Lp and Ls. This implies that, when misalignment between the primary and secondary magnetic couplers occurs, more than nominal power is transferred, and hence regulation is required.

Conventionally, power is regulated by controlling the amplitude of the fundamental voltage applied across the secondary compensation network. However, in the case of the BAB, by symmetrically increasing the duty cycle of both inverter legs, the DC voltage on each inverter leg and the magnitude of the fundamental voltage applied across the secondary compensation network (V_{si}) can be reduced. Controlling both these variables with just one control input is more efficient, as a smaller change in duty cycle will result in larger reduction in power. This characteristic is illustrated by Fig.5, which displays voltage waveforms for three different duty cycles.

Figures 5a-5e show other alternative modulation techniques which may be used. In these figures the relevant voltages shown in Figure 5 are not illustrated. However, the switching

patterns which result in a combined duty cycle for each of SA and SB are illustrated, along with the resultant output VSI.

Experimental Results

As discussed above with reference to Figure 3, an active bridge primary and boost active bridge secondary configuration (AB-BAB) should regulate the output power more efficiently when compared to a standard IPT system employing conventional switch-mode converters. This was verified experimentally using the test set ups specified in Table I and Table II. In the case of the conventional system, which employed active bridges in primary and pick-up, power was regulated by driving each inverter leg on the secondary side at a constant 50% duty cycle and modulating the phase angle between them. The AB-BAB utilised the aforementioned regulation technique. Efficiency data was obtained for each configuration at varying levels of regulation. The data recorded using a Yokogawa WT1800 power analyser is shown below in Fig. 6. It is clear that when output power is regulated to below rated power the AB-BAB configuration is superior in terms of efficiency. Moreover, the AB-BAB configuration is up to 10% more efficient at very light loads.

TABLE I

Parameters of DAB experimental setup

DAB Device/ component/ Parameter	Part #/ Value
MOSFET	C3M0065090D
V_{in} & V_{out}	150V
L_p	184.7uH
L_s	185.8uH
C_p	18nF
C_s	18nF
Switching frequency	85kHz
Z height	160mm
Unregulated power	700.6W

TABLE 2

Parameters of DAB experimental setup

DAB Device/ component/ Parameter	Part #/ Value
MOSFET	C3M0065090D
V_{in} & V_{out}	150V

L_p	199.6uH
L_s	199.6uH
C_p	18nF
C_s	18nF
M	80uH
L_a & L_b	750uH
C_a & C_b	940uF
Switching frequency	85kHz
Z height	100mm
Unregulated power	721.6W

Example #2: Grid integration of a Bi-Directional IPT system utilising a DBAB for vehicle to grid/grid to vehicle applications

Vehicle to grid/grid to vehicle (V2G/G2V) systems have been proposed to provide many beneficial services to the utility grid. The main benefit is the ability to access the increased energy storage capability provided by EV's. This is especially useful when power systems are heavily reliant on renewable energy generation, as fluctuations in power generation can be absorbed by EV batteries. This ensures grid voltage stability. Furthermore, V2G/G2V systems can provide other grid services such as the ability to inject reactive power and harmonics into the grid, resulting in an improved grid power factor, efficiency and stability. Conventionally, a grid tied converter, which is responsible for grid current regulation, feeds an inverter, which drives an isolation technology (IPT is used as the isolation technology in this example). However, a large storage capacitor is required in such a system to decouple the power ripple resulting from single-phase grid, and the DC power supplied to the EV battery. Hence a bulky and expensive electrolytic capacitor is placed at the DC-link between the grid tied converter and the inverter. Moreover, due to the low voltage rating of electrolytic capacitors, the DC link voltage is limited to well below the voltage rating of wide bandgap devices.

Referring to Figure 7, an example is shown which illustrates how a DBAB based grid connected bi-directional IPT (BD-IPT) system for V2G/G2V applications can overcome the aforementioned problems. The proposed configuration also requires a grid-tied converter, but a large electrolytic capacitor is no longer required on the DC link. This is because, the voltage across the inverter leg DC capacitors (C_{pa}, C_{pb}, C_{sa}, C_{sb}) can be actively controlled through duty cycle modulation (as described in the preceding example above). Hence, energy can be stored or extracted out of these capacitors, allowing for the absorption of the

mains frequency power ripple. Furthermore, the high DC voltage and large voltage ripple on these capacitors reduce the overall capacitance requirement, permitting the use of film capacitors.

This system was simulated in MATLAB/PLECS using the parameters described in Table III. A series-series compensation network, and the coupling topology Fig.4, (b) was chosen. The results of this simulation are illustrated in Fig. 8, where graph (a) shows the soft DC-link voltage and also the voltage boosting characteristic of the BAB. Graph (b) shows the grid voltage and current, however, the grid current is not regulated by the grid-tied converter as with a conventional system.

In this system the grid-tied converter is simply an active rectifier and the grid current is regulated by the primary converter by modulating the phase angle between the two converter legs as discussed in the previous example. Graph (c) displays the voltage modulation on C_{sa} and C_{sb} required to absorb the low frequency power ripple. The boosting characteristic of the converter is shown again, as the average capacitor voltage is at twice the EV battery voltage. The result of this modulation is shown in graph (d), the higher frequencies present in the output power can be attributed to the voltage modulation of the DC side capacitors.

TABLE III

Parameters of DAB simulation setup

DAB Device/ component/ Parameter	Part #/ Value
MOSFET	C3M0065090D
V_{grid}	230V
C_{dc}	10uF
C_{pa} & Cp_b	1uF
C_{sa} & C_{sb}	250uF
C_p & C_s	17.5nF
L_p	199.58uH
L_s	199.61uH
M	99.7uH
Switching frequency	85kHz
P_{out}	700.6W

Example #3: IPT technology based dynamic EV charger.

Electric vehicles are an emission free alternative to conventional vehicles. However, the energy density of battery technology available today lead to frequent and time-consuming charging requirements.

Dynamic EV charging will help reduce energy storage requirements in EV's, as charging can take place while driving the vehicle. Dynamic charging requires multiple primary magnetic couplers to be placed under the surface of the road. Each coupler (or few couplers) typically requires its own primary converter and each primary converter requires a supply. A cost effective solution is to provide a DC voltage distribution network, which eliminates the requirement of multiple grid-tied converters.

Such a situation is shown in Fig. 9. For safety and compatibility reasons, the DC voltage network would operate at approximately 380V to 400V which may become a standard for low voltage DC distribution. Due to the much higher peak power required to be delivered by a dynamic charging system, primary magnetic coupler currents will be very high if supplied with a low voltage source. Higher currents lead to undesired heating of the magnetic coupler, which is further exacerbated by the lack of any airflow. However, if a BAB topology is used as the primary converter, the primary magnetic coupler can operate at twice the voltage of the DC distribution system reducing heating affects due to lower current and improving overall system efficiency.

Example #4

Figure 10 shows another example showing IPC system in which the primary power supply comprises a boost active bridge converter as described above, but the secondary is 50 is simplified having diodes D5 to D8 rather than switches. Other aspects of the BAB topology remain the same in the secondary. The use of simple diode rectifiers enables the pick-up to be simplified, and is appropriate where only uni-directional power flow from the primary to the secondary is required. The wave forms in the pick-up in this example is similar to that observed with the original examples described elsewhere in this document. However, if pick-up power needs to be regulated then a regulator will be required following the rectifier.

BAB Converter configuration description

The proposed BAB technology can replace the VSI found in commonly used uni or bi-directional IPT systems regardless of the compensation topology and the type of magnetic coupler employed. However, to highlight all the benefits of the BAB technology, including its ability to inherently eliminate circulating currents, an LCL tuned BD-IPT system, which utilises

BAB's as both the primary and secondary inverters, shown in Fig. 11 (similar example as figure 7 or 10), is considered as an example in this example. The primary BAB of this system drives the primary magnetic coupler, Lpt, through Lpi and Cp, which together forms an LCL compensation network. Similarly, the secondary is composed of a BAB and an LCL network formed by Lst, Cs and Lsi. In a typical application, the supply to the primary BAB is derived through a grid tied inverter. For simplicity, the DC link voltage generated by this grid tied inverter is modelled by a DC voltage source, Vp. The secondary BAB will be directly connected to the EV battery, which is modelled by Vs.

Since the electronics on the primary and secondary side are identical, the operating principles discussed below pertain to both sides. However, to ensure generality, subscript x is used, x ∈ {p, s} where subscripts p and s represent the primary and secondary side, respectively. Each side consists of two halfbridges; half-bridge a, Bxa, which is made up from switch pair SxaT and SxaB; and half-bridge b, Bxb, which is made up from switch pair SxbT and SxbB. Vx is connected to both, Bxa and Bxb through inductors Lxa and Lxb, respectively. The capacitors Cxa and Cxb, are connected across the DC sides of Bxa and Bxb, respectively. This arrangement forms an interleaved buck-boost converter between Vx and Cxa; as well as Vx and Cxb. The combination of Bxa and Bxb also form a quasi-full-bridge inverter, whose output, vxi, drives the corresponding LCL network.

Bxa and Bxb are switched in a complementary manner at fs, which is equal to, or in proximity to, the resonant frequency of the two LCL networks, f_T . As a result, the output voltages, vxa, produced by Bxa, and vxb, produced by Bxb, are 180 degrees out of phase. The duty-cycles of vxa and vxb are defined as Dxa and Dxb, respectively. Since the average of vxa and vxb should be equal to Vx at steady-state, the voltages VCxa and VCxb are a function of Dxa and Dxb, respectively, as given by,

$$V_{Cxa}D_{xa} = V_{Cxb}D_{xb} = V_x \tag{3}$$

Equation (3) shows, that a nominal duty-cycle of 50% doubles Vx, and reducing/increasing the duty-cycle, results in a higher/lower voltage across each half-bridge, as depicted in Fig. 12. Figures 12(a) - (c) illustrate the Voltages produced by the BAB model utilising the proposed switching scheme at (a) Dx = 50%, (b) Dx = 60% and (c) Dx = 40%

The output of the quasi-full-bridge converter, vxi, is the difference between voltages vxa and vxb, and is also depicted in Fig. 12. As such, Bxa and Bxb are normally operated with equal

duty-cycles to produce a symmetric vxi, and the duty-cycle of each side can be referred to as simply Dx i.e. Dxa = Dxb = Dx. Similar to the control strategies proposed in :

$$V_{pr} = j\omega_s M I_{st} \text{ and } V_{sr} = j\omega_s M I_{pt} \quad (4)$$

the RMS value of vxi, produced by the BAB, can be controlled using phase-shift modulation, while Dx is set to 0.5. However, the proposed BAB can also be controlled by modulating Dx, while Bxa and Bxb are driven 180 degrees out of phase. As shown in Fig 12, increasing Dx beyond 0.5, lowers the RMS value of vxi, by increasing the duration of 0 V level, , as well as reducing the amplitude of vxi. Therefore, in contrast to traditional phase-shift modulation scheme, the new duty-cycle control scheme employed by the BAB, will reduce the control effort required and facilitate zero voltage switching (ZVS) of devices over a wider load range. Furthermore, the magnitude of vxi can be increased by operating at a Dx below 0.5, in order to compensate for reduced power transfer under misaligned conditions or drop in DC-link voltage. Although decreasing Dx below 0.5 increases, as per (1) the amplitude of vxi increases, resulting in a net increase in the RMS value of vxi. is a function Dx as given by,

$$\alpha_x = \begin{cases} \pi - 2\pi D_x & D_x \leq 0.5 \\ \pi - 2\pi(1 - D_x) & D_x > 0.5 \end{cases} \quad (5)$$

Due to non-ideal conditions, a conventional full-bridge converter that is controlled using phase-shift modulation, may generate an output voltage with a slight DC offset. As mentioned previously, this DC offset will lead to a large circulating DC current through the inductors of an LCL tuned BD-IPT system. To resolve this issue, a DC blocking capacitor is normally placed in series with one of the inductors, adding to system cost and size. However, in the BAB, as given by (1), the two capacitors employed across each half-bridge self-adjust VCxa and VCxb to eliminate the DC offset of vxi. Therefore, as evident from Fig. 11, the proposed BD-IPT system does not employ DC blocking capacitors.

The following model elaborates upon the power transfer characteristics, component stresses and efficiency, of the proposed system. Figures 13 depicts an equivalent phasor domain representation of the LCL networks. Typically, to minimise the VA rating of the converters and to maximise the power transfer, both LCL networks are tuned to f_T .Therefore,

$$(2\pi f_T)^2 = \omega_T^2 = \frac{1}{L_{pi}C_p} = \frac{1}{L_{pt}C_p} = \frac{1}{L_{si}C_s} = \frac{1}{L_{st}C_s}. \quad (6)$$

However, in EV charging applications, misalignment between magnetic couplers invariably results in changes to the self-inductances, Lpt and Lst, detuning the LCL networks. Moreover, in some cases, at the cost of converter VA rating, the networks are intentionally de-tuned to present a slightly inductive input impedance at the switching frequency, fs ($\ll_s$), to ensure a wide ZVS range.

In contrast to a traditional full-bridge based BD-$_s$IPT system, the output power of the proposed BAB based system, is a function of control variables, Dp and Ds, as well as $_p$ and $_s$. Nominally, the converters are operated with Dp = Ds = 50%, when delivering rated power. Under these conditions, accordingly with equation (5), being a function Dp and Ds, both $_p$ and $_s$ are 0, respectively. As discussed in the previous section, the output power can be regulated by controlling Dp and Ds. Increasing one or both of the duty-cycles above 50% results in reduced output power. However, increasing Dp and/or Ds also leads to in an increase in $_p$ and/or $_s$. Thus, even a small increase in the duty-cycles translates to a much larger reduction in output power, enabling the converter to maintain ZVS conditions over a wider load range. Unlike in traditional BD-IPT systems, the output power of the proposed BAB based system can be increased by decreasing one or both of the duty-cycles below 50% to compensate for variations in system parameters.

The operating region of the proposed converter can be selected based on the symmetry of the circuits and the desired output power range. For example consider a symmetric system, whose input and output supply voltages are equal and so are the primary and secondary coil quality factors. Therefore, the condition for minimising conduction losses in the compensation networks is Dp = Ds. Thus, based on this condition, the desired region of operation is highlighted by the red line in the figure 14. The nominal operating point is chosen such that it meets the rated power of the system and to provide enough head room to increase the primary or secondary VA in case of input/output voltage changes or coupler misalignments. The practical limit of the primary and secondary VA's are defined by the regions shaded in grey.

To achieve high overall efficiency over the entire load range, the converter should be designed to ensure ZVS operation over the desired region of operation. The ZVS Range of the proposed converter is a function of the converter switching frequency, compensation network tuned frequency, the value of the DC inductors and the output power. However, since the switching frequency and the output power range are usually constrained, the ZVS range of the converter can be adjusted by either changing the compensation network tuning or the value of the DC inductors.

Consider the system discussed above, operating with a switching frequency of 85 kHz, a tuned frequency of 87 kHz and the DC inductors all designed to 430 uH. The ZVS range of this system is shown in Figure 15. Clearly, the converter is hard switched during a large proportion of the desired region of operation. Therefore, the tuned frequency can be adjusted

to 88 kHz and the DC inductor values to 170 uH. The resulting ZVS range is shown in Figure 16.

Maximum Efficiency Tracking

Power loss associated with ipt and ist accounts for a significant proportion of total power loss in a typical BD-IPT system. Thus, to maximise the power transfer efficiency, as discussed in [23], the losses in the couplers are matched. This can be achieved by controlling ipt and ist, such that $i^2_{pt} r_{pt} = i^2_{st} r_{st}$, and is referred to as impedance matching by controlling the operating Q. For example, consider a symmetric system, where primary and secondary circuits are identical. Output power normalised to rated output power of this system, as function of Dp and Ds, is shown in Figure 17. In this example, when delivering rated power, efficiency would be maximised by operating at point A. However, consider an asymmetric case when Lst is physically smaller but has the same self-inductance as Lpt, which is often the case for EV charging applications. Typically, a smaller coupler implies higher resistive losses due to the reduced winding area. As such, to maximise power transfer efficiency while still delivering rated power, the operating point can be shifted towards B to increase ipt and reduce ist. Similarly, consider another example, where the EV battery voltage is increasing as it charges at a constant power level. The operating point, which is close to point C when the battery is depleted, can be shifted towards point B during the charge process in order to maximise power transfer efficiency. In contrast, impedance matching is typically achieved at the expense of efficiency and power transfer capability in a traditional full-bridge converter based BD-IPT system.

Reduced Conduction Losses

The conduction losses associated with the BAB based system can be divided into conduction losses in the switches, LCL networks and the DC inductors. In comparison to a traditional full-bridge based BD-IPT system, under nominal operating conditions, the primary and secondary LCL networks are driven at twice Vp and Vs, respectively, halving the currents in the LCL networks. Thus, although a higher magnetic coupler inductance is required to achieve the same level of power transfer, effectively the conduction losses in the LCL networks are lowered by about 70% . Whereas, due to the addition of the currents flowing through the DC inductors, the currents through the top and bottom switches of each half-bridge are asymmetric, leading to unevenly distributed switch conduction losses. the switch conduction losses. In the present case the switch conduction losses of the BAB are lowered by approximately 50%. Since the secondary of the proposed system utilises a BAB, the switch conduction losses of the secondary are also significantly reduced. The additional losses associated with the DC inductors used by the BAB's of the proposed system are

significantly lower in comparison to the reduction in conduction losses of the switches and LCL networks. As a result, the overall efficiency is improved.

Reduced current ripple

As the two half-bridges together with the two DC inductors of each BAB forms two identical interleaved buck-boost converters, the switching frequency current ripple present in Ip and Is is greatly reduced. Under nominal operating conditions, ∀Ip_pk is zero. As the duty-cycle deviates from 50%, ∀Ip_pk increases and Ip appears to be at twice the switching frequency. However, it is comparatively lower in amplitude than $\forall I_{Lpa_pk}$ under all operating conditions. Similarly, the ripple current present in Is on the secondary BAB is also reduced.

Example #5

In order to illustrate the viability of the proposed system as well as to validate the mathematical models developed, a 3.5 kW prototype was designed and built. Circuit parameters of this prototype system are listed in Table IV. Since Vp is 280 V, under nominal operating conditions where Dp is 50%, in accordance with (1), the amplitude of v_{pi} is approximately 560 V. This is evident from Fig. 12 (b), which depicts the experimental waveforms of vpa, vpb and vpi. When Dp is increased to 60%, as shown by Fig. 12 (a), the amplitude of vpi is lowered to 467 V and $_p$ is increased, resulting in an overall reduction in Pout. The system's ability to compensate for a low input voltage was also simulated by reducing Vp to 250V and setting Dp to 40%. Although this resulted in an increase in p, the amplitude of vpi was increased to 595 V as shown by Fig. 12 (c), hence delivering rated power to the load.

Steady-state waveforms captured from the prototype for various operating conditions were compared to theoretical waveforms. For example, experimental waveforms obtained when BAB's are operated at a duty-cycle of 50% and 60% are compared with theoretically obtained waveforms in Figure 18 and Figure 19, respectively. As evident, the experimental and theoretical waveforms present excellent correlation. It is also evident from ipi and isi waveforms, that operating at 60% duty-cycle lowers power transfer.

Figure10 displays Ip, iLpa and iLpb, at 40%, 50% and 60% duty-cycles. Theoretical peak inductor currents can be calculated as 9.3 A, 8 A, and 5.6 A, under 40%, 50%, and 60% duty-cycle operation, respectively. The experimental results shown in Fig.20, closely matches these theoretical values. Moreover, as evident from Fig.20 (b), ∀Ip_pk is nearly zero when operated at 50% duty-cycle. Furthermore, ∀Ip_pk when operated at a duty-

cycle of 40% and 60% can be calculated as 0.7 A and 0.5 A, respectively, which is experimentally verified in Fig.20.

Fig. 21 depicts the efficiency of the prototype as a function of Pout. Pout was regulated by adjusting both Dp and Ds equally. Varying the duty-cycle from 50% to 80% resulted in a power variation from 3.5 kW to 0.5 kW, respectively. As evident, the efficiency is approximately constant throughout the entire load range with a minimum of 94.9% at 1.2 kW and a maximum of 95.4% at 2.2 kW. In order to verify the improved performance of the proposed BAB based system, efficiency of a traditional full-bridge based BD-IPT system was compared over the same load range. The traditional system used for comparison employed the same magnetic couplers and the full-bridge converters derived power from the same 280 V DC sources. DC-blocking capacitors, Cpt and Cst, placed in series with the magnetic couplers, were also used to ensure 3.5 kW is delivered to the load when operated under nominal conditions. The output power of the system is regulated utilizing phase-angle modulation.

TABLE IV

Parameters of BAB experimental setup

Parameter	BAB system	Full-bridge system
V_p & V_s	$280\,V$	$280\,V$
L_{pt}	$43.4\,\mu H$	$43.4\,\mu H$
L_{pi}	$40.3\,\mu H$	$21.2\,\mu H$
C_p	$74.3\,nF$	$152.4\,nF$
L_{st}	$46.28\,\mu H$	$46.28\,\mu H$
L_{si}	$42.3\,\mu H$	$21.2\,\mu H$
C_s	$69.66\,nF$	$149\,nF$
C_{pi}	—	$155\,nF$
C_{st}	—	$142.7\,nF$
L_{pa}	$434\,\mu H$	—
L_{pb}	$434\,\mu H$	—
L_{sa}	$434\,\mu H$	—
L_{sb}	$434\,\mu H$	—
k	0.36	0.36
$Airgap$	$150\,cm$	$150\,cm$
f_T	$85\,kHz$	$85\,kHz$
MOSFET	$C3M0065090D$	$C3M0065090D$

Table IV, lists the parameters of this system. As evident from Figure 21, the full-bridge based system achieves a maximum efficiency of 94.3% when delivering 3.5 kW. However, the efficiency drops sharply to 89.3% as the output power is reduced to 0.5 kW. Overall, these results prove not only the superiority of the BAB technology in terms of efficiency, but also

the greater flexibility to operate over a wide load range without the concern for lowered efficiency.

A novel power converter, named a Boost Active Bridge (BAB), to replace the full-bridge converters is presented. In order to fully exploit the capabilities of the proposed converter, a novel switching scheme was also presented. A comprehensive mathematical model that predicts steady-state currents, voltages and power transfer was also presented to highlight the key advantages of the BAB technology. One of the main advantages of the present BAB converter is its ability to operate at twice the input voltage and thus reducing conduction losses in the system. A higher voltage also provides an opportunity to effectively utilise wide bandgap devices, which are known for their high efficiency. Also, the converter of the present invention eliminates the issue of DC offset currents that may cause undesirable issue such as core saturation. Thus for example the need for AC coupling capacitor used in traditional system can be eliminated further improving the efficiency and reliability while lowering the cost.

A conventional system, which utilises a dual active bridge, lacks the capability to utilise wide bandgap devices to their full voltage rating. This limitation can be mainly attributed to limited supply and output voltages found in a typical application. Increasing the operating voltage of these systems can be a simple, yet expensive solution. For example, additional power converters can be used to boost/buck supply/load voltages, however an increased component count and reduced efficiency lead to an undesired solution. The converter of the present invention is an inexpensive solution which is capable of fully utilising the voltage rating of wide bandgap devices. The present BAB topology also offers all the advantages of additional pre/post regulating stages without the need for any extra switching devices.

The viability of the system has been verified through the development of a 3.5 kW prototype system. The experimental results prove that the proposed system offers a higher power transfer efficiency throughout the entire load range in comparison to a traditional full-bridge based system. The experimental results also validate further advantageous properties of the proposed system such as the elimination of the DC-blocking capacitor, the ability to track maximum efficiency over a wide range of system parameters and reduced current stresses in the components. Furthermore, the experimental results demonstrate a substantial improvement in efficiency under all operating conditions, validating the viability of the proposed converter.

Throughout the description like reference numerals will be used to refer to like features in different embodiments.

Unless the context clearly requires otherwise, throughout the description, the words `comprise¸ `comprising¸ and the like, are to be construed in an inclusive sense as opposed to an exclusive or exhaustive sense, that is to say, in the sense of `including, but not limited to¸.

Although this invention has been described by way of example and with reference to possible embodiments thereof, it is to be understood that modifications or improvements may be made thereto without departing from the scope of the invention. The invention may also be said broadly to consist in the parts, elements and features referred to or indicated in the specification of the application, individually or collectively, in any or all combinations of two or more of said parts, elements or features. Furthermore, where reference has been made to specific components or integers of the invention having known equivalents, then such equivalents are herein incorporated as if individually set forth.

In the foregoing Detailed Description, various features are grouped together in a single embodiment to streamline the disclosure. This method of disclosure is not to be interpreted as reflecting an intention that the claimed embodiments of the inventive subject matter require more features than are expressly recited in each claim. Rather, as the following claims reflect, inventive subject matter lies in less than all features of a single disclosed embodiment. Thus, the following claims are hereby incorporated into the Detailed Description, with each claim standing on its own as a separate embodiment.

It will be readily understood to those skilled in the art that various other changes in the details, material, and arrangements of the parts and method stages which have been described and illustrated in order to explain the nature of the inventive subject matter may be made without departing from the principles and scope of the inventive subject matter as expressed in the subjoined claims.

Any discussion of the prior art throughout the specification should in no way be considered as an admission that such prior art is widely known or forms part of common general knowledge in the field.

We Claim

1. An AC-AC converter comprising:
   a bridge circuit having a first leg and a second leg, each leg including a high switch and a low switch, the high switches being connected to a first energy source and the low switches being connected to ground,
   a coupling network(s) having a first connection between the switches of the first leg and a second connection between the switches of the second leg,
   a second (or multiple secondary) energy source(s) connected between the coupling network(s) and ground.

2. The AC-AC converter as claimed in claim 1 wherein the first energy source comprises a capacitive member.

3. The AC-AC converter as claimed in claim 1 or claim 2 wherein a separate energy source is connected between each high switch and ground.

4. The AC-AC converter as claimed in any of the preceding claims 1 to 3 wherein a third energy source is connected in parallel with a coupling network.

5. The AC-AC converter as claimed in any of the preceding claims 1 to 4 wherein the coupling network comprises one or more inductors or capacitors arranged to interface the second or third energy source effectively with the first and second legs.

6. The AC-AC converter as claimed in any of the preceding claims 1 to 5 wherein the coupling network may comprise a first inductive element connected between the second energy source and the switches of the first leg, and a second inductive element connected between the second energy source and the switches of the second leg.

7. The AC-AC converter as claimed in any of the preceding claims 1 to 6 wherein the first and second inductive elements are coupled.

8. The AC-AC converter as claimed in any of the preceding claims 1 to 7 wherein a third inductive element may be connected between the first and second inductive elements and the second energy source.

9. The AC-AC converter as claimed in any of the preceding claims 1 to 8 further comprising a control means to control the switches of the AC-AC converter.

10. The AC-AC converter as claimed in any of the preceding claims 1 to 9 wherein the control means is also configured to control the duty cycle and/or phase of the switches.

11. The AC-AC converter as claimed in any of the preceding claims 1 to 10 wherein the control means may have one or more input control variables as inputs for controlling the switches.

12. The AC-AC converter as claimed in any of the preceding claims 1 to 11 wherein the control of the duty cycle of the switches can control two output variables of the converter.

13. The AC-AC converter as claimed in any of the preceding claims 1 to 12 wherein the control means is configured to control energy transfer between each energy source(s) to optimise the efficiency and power transfer of the converter.

14. The AC-AC converter as claimed in any of the preceding claims 1 to 13 wherein the controller may control the duty cycle of the legs symmetrically.

15. The AC-AC converter as claimed in any of the preceding claims 1 to 14 further comprising a dual bridge converter comprising two converters wherein the AC energy sources are coupled to each other.

16. The AC-AC converter as claimed in any of the preceding claims 1 to 15 further comprising a capacitive element connected between each high switch and ground.

17. An IPT converter comprising:
a bridge circuit having a first leg and a second leg, each leg including a high switch and a low switch, the high switches being connected to a first energy source and the low switches being connected to ground,
a coupling network(s) having a first connection between the switches of the first leg and a second connection between the switches of the second leg,
a second energy source connected between the coupling network and ground (directly or through a another coupling network), and
a magnetic coupler connected in parallel with the coupling network(s).

18. The IPT converter as claimed in claim 17 wherein the magnetic coupler includes a coil which may be series or parallel tuned.

19. The IPT converter as claimed in claim 17 or claim 18 wherein the magnetic coupler further comprises a primary apparatus or a secondary (pick-up) apparatus,

20. The IPT converter as claimed in any one of the preceding claims 17 to 19 wherein the magnetic coupler is configured for bi-directional power transfer.

21. A method of controlling an AC-AC converter, the method comprising the steps of: controlling the bridge switches to alternately apply current from a first energy source to a coupling network which couples the converter to a second energy source, and controlling the duty cycle of the or selected bridge switches to control the voltage across a third energy source connected in parallel with the coupling network.

22. A method of controlling the AC-AC converter as claimed in claim 21 wherein the energy flow between first, second and third energy sources is bi-directional.

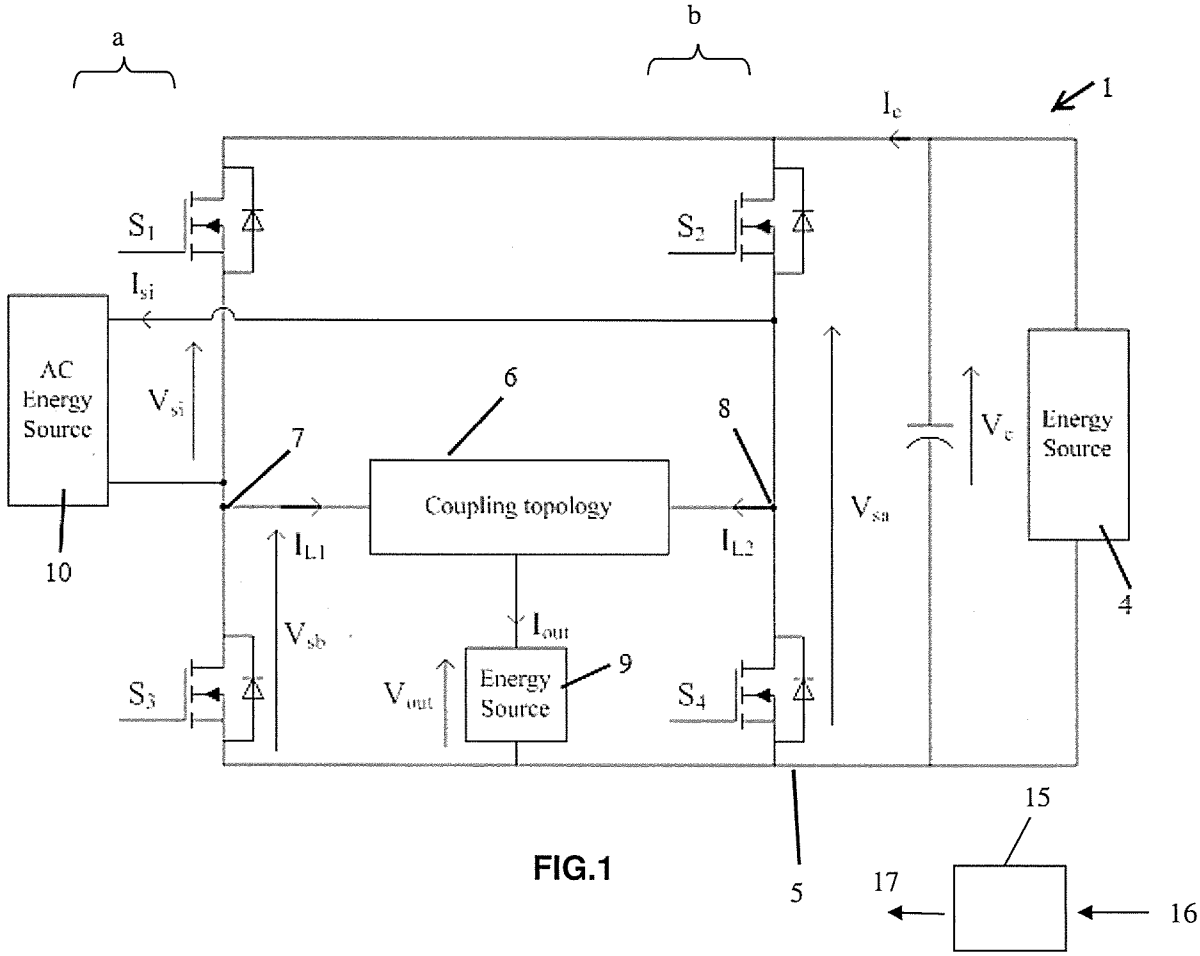

a
b
1
I_e
S_1
S_2
I_{si}
AC Energy Source
V_{si}
6
7
8
Coupling topology
V_c
Energy Source
V_{sa}
I_{L1}
I_{L2}
10
4
V_{sb}
I_{out}
S_3
V_{out}
Energy Source
9
S_4
15
17
16
5

FIG.1

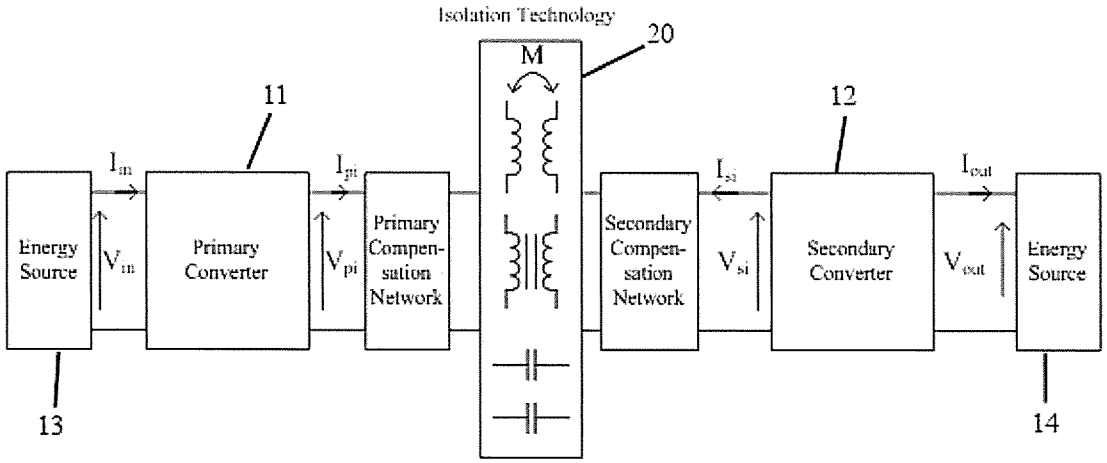

Isolation Technology
20
M
11
12
I_{in}
I_{pi}
I_{si}
I_{out}
Energy Source
V_{in}
Primary Converter
V_{pi}
Primary Compen-sation Network
Secondary Compen-sation Network
V_{si}
Secondary Converter
V_{out}
Energy Source
13
14

FIG.2

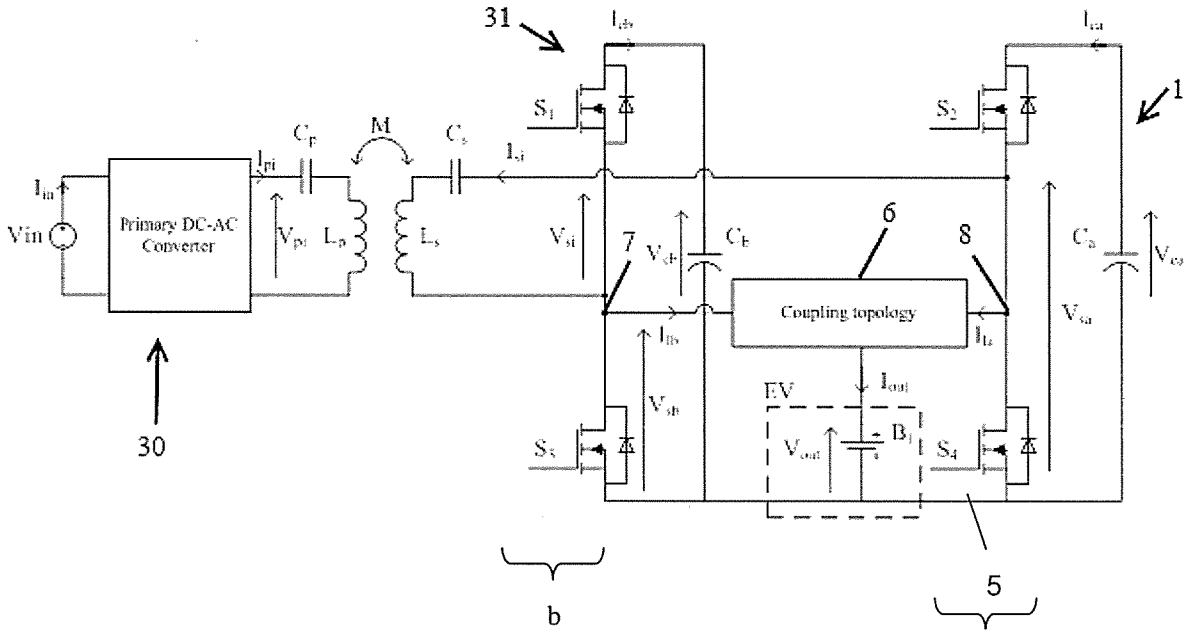

31
1
Primary DC-AC Converter
Vin
30
Coupling topology
EV
6
7
8
5
b
a

FIG.3

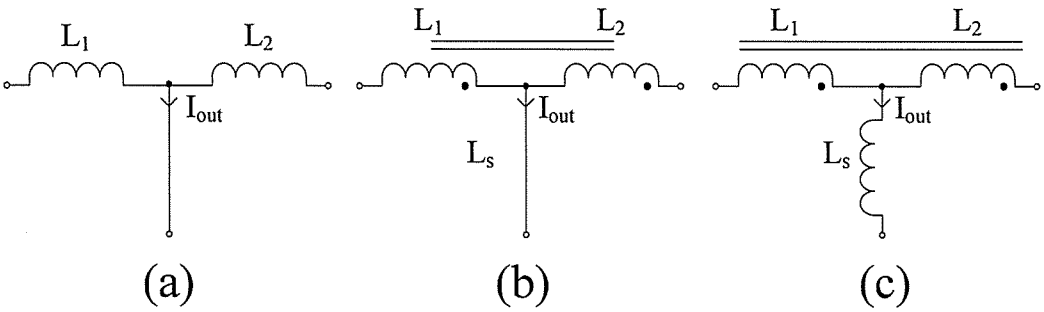

L1
L2
Iout
Ls
(a)
(b)
(c)

FIG.4

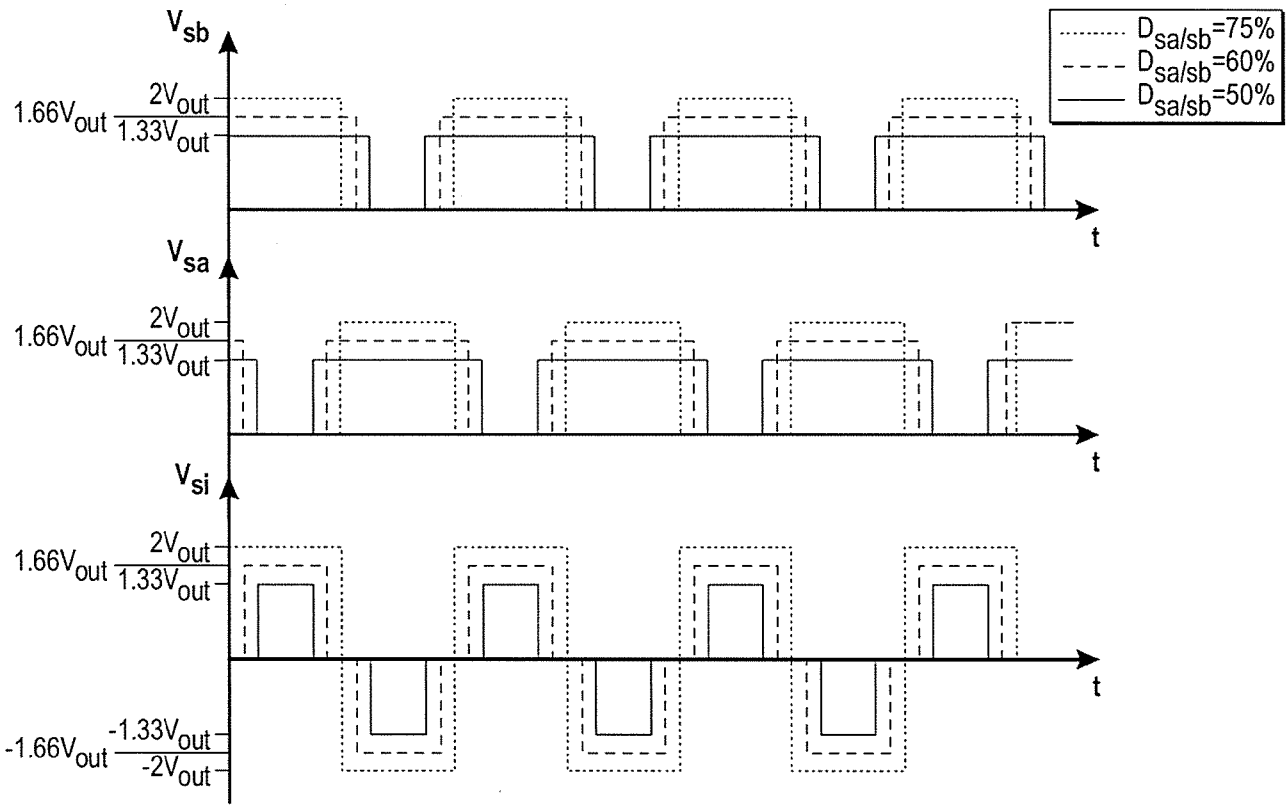

V_{sb}
$2V_{out}$
$1.66V_{out}$
$1.33V_{out}$
t
V_{sa}
$2V_{out}$
$1.66V_{out}$
$1.33V_{out}$
t
V_{si}
$2V_{out}$
$1.66V_{out}$
$1.33V_{out}$
t
$-1.33V_{out}$
$-1.66V_{out}$
$-2V_{out}$
$D_{sa/sb}$=75%
$D_{sa/sb}$=60%
$D_{sa/sb}$=50%

FIG.5

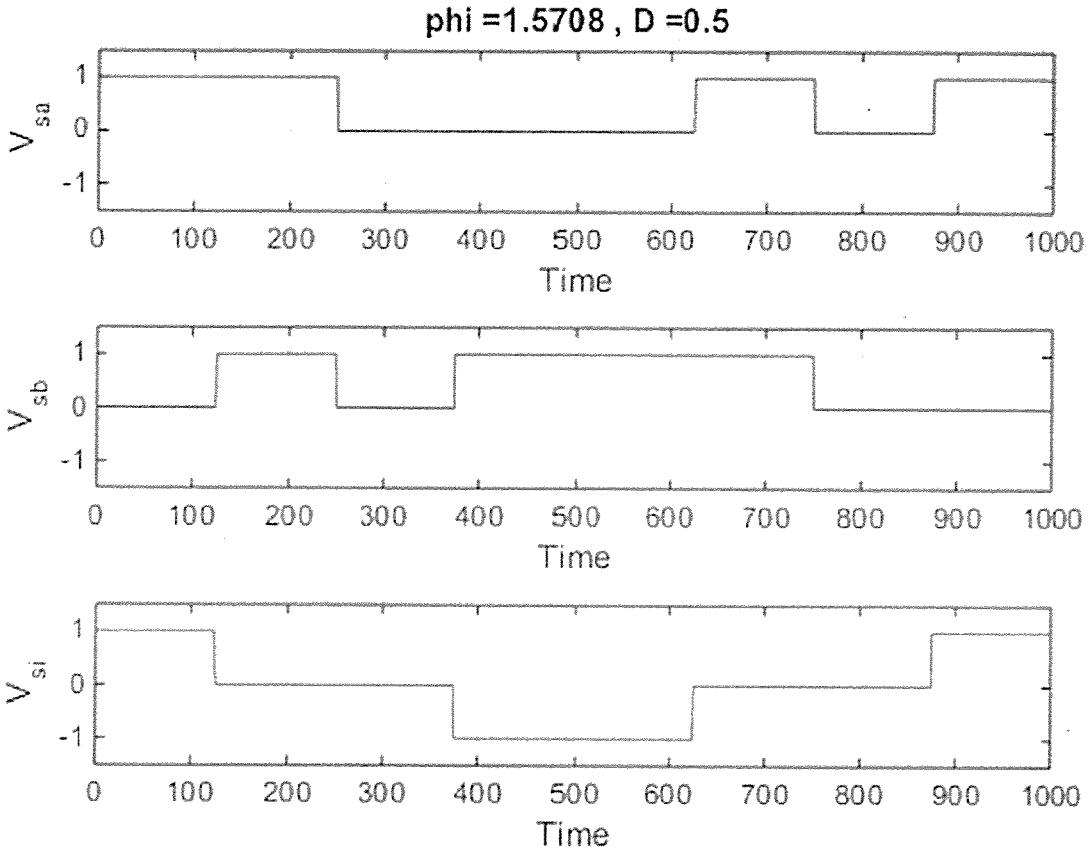

phi =1.5708 , D =0.5
V sa
V sb
V si
1
0
-1
0 100 200 300 400 500 600 700 800 900 1000
Time

FIG.5A

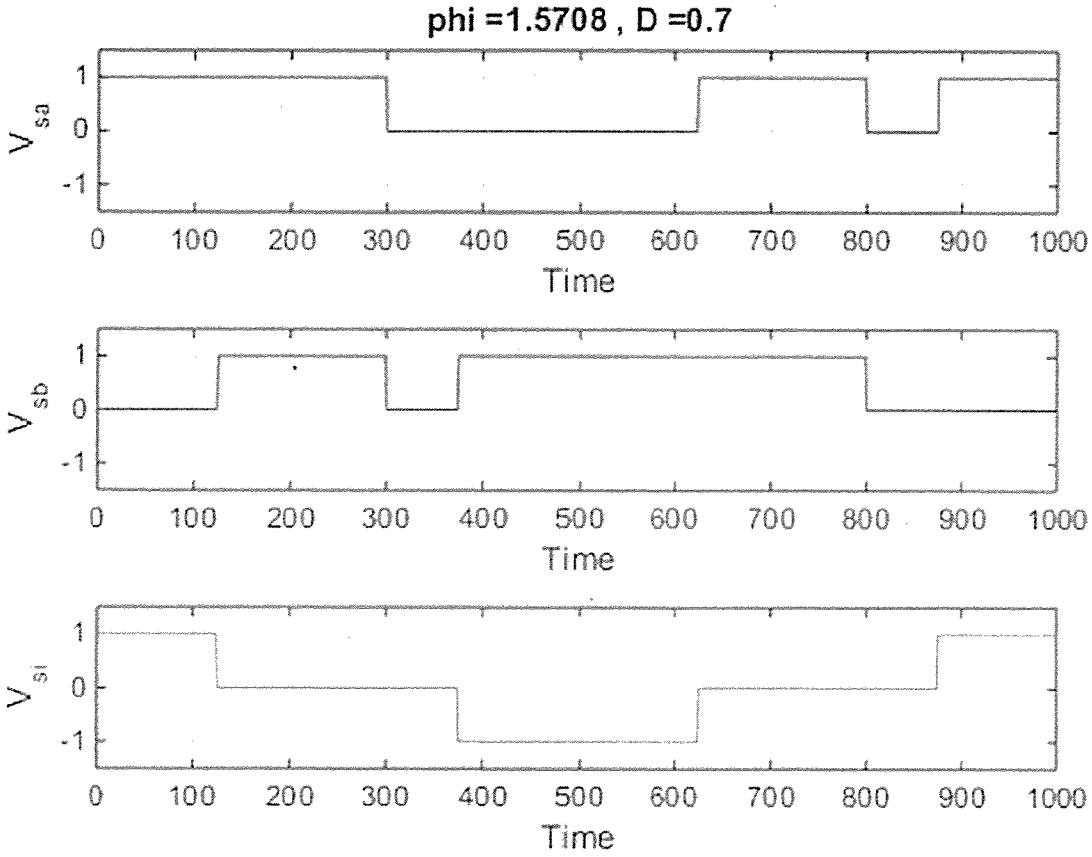

phi =1.5708 , D =0.7
V sa
V sb
V si
1
0
-1
0 100 200 300 400 500 600 700 800 900 1000
Time

FIG.5B

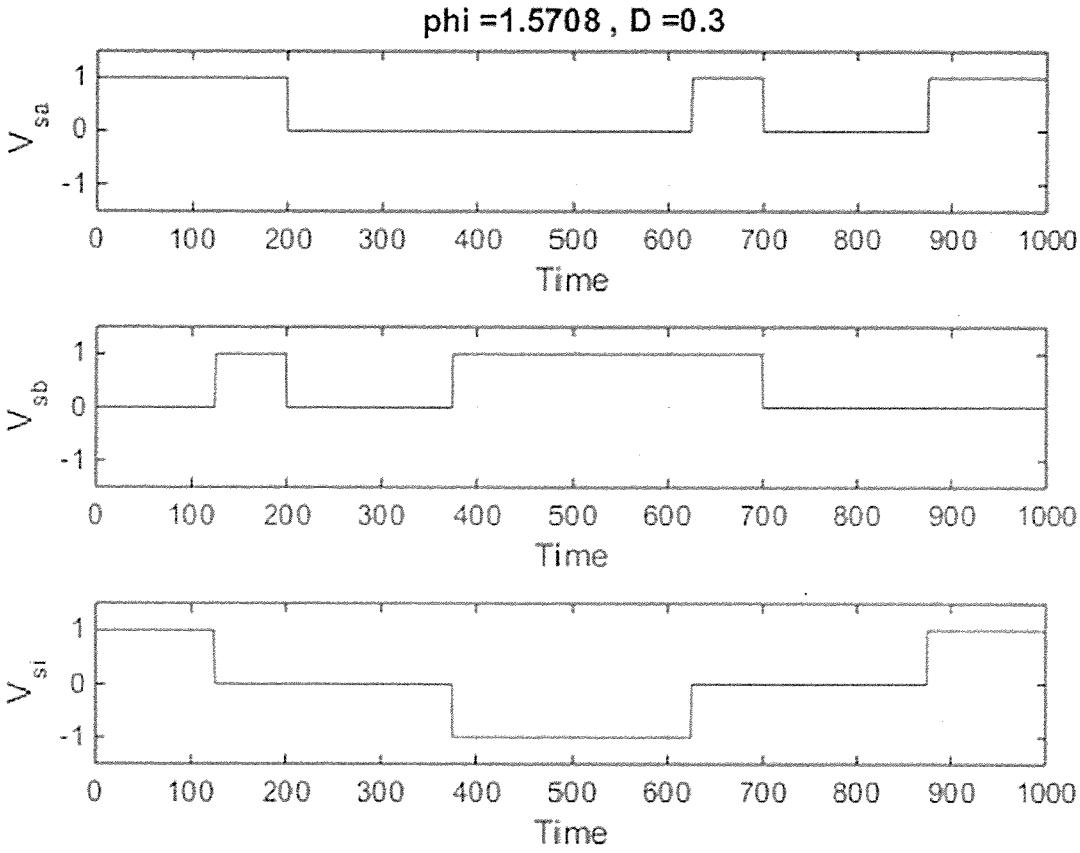

phi =1.5708 , D =0.3
V_{sa}
V_{sb}
V_{si}
1
0
-1
0
100
200
300
400
500
600
700
800
900
1000
Time

FIG.5C

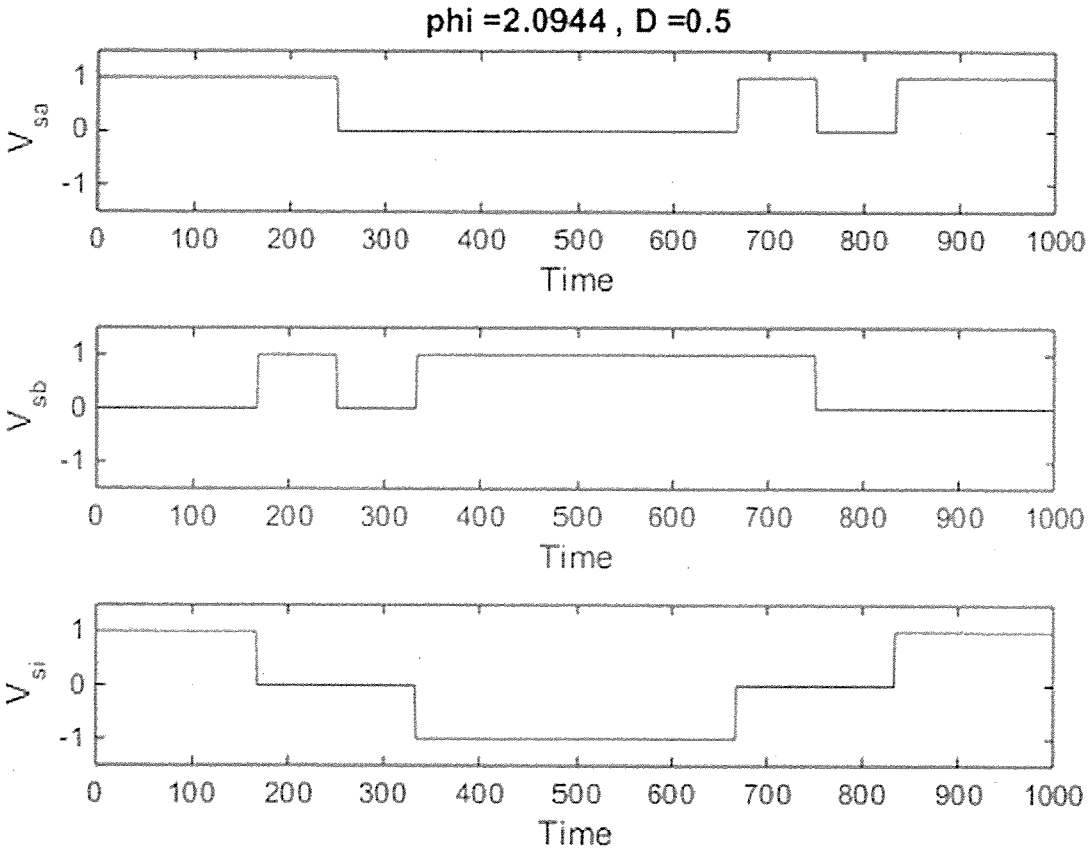

phi =2.0944 , D =0.5
V_{sa}
V_{sb}
V_{si}
1
0
-1
0 100 200 300 400 500 600 700 800 900 1000
Time

FIG.5D

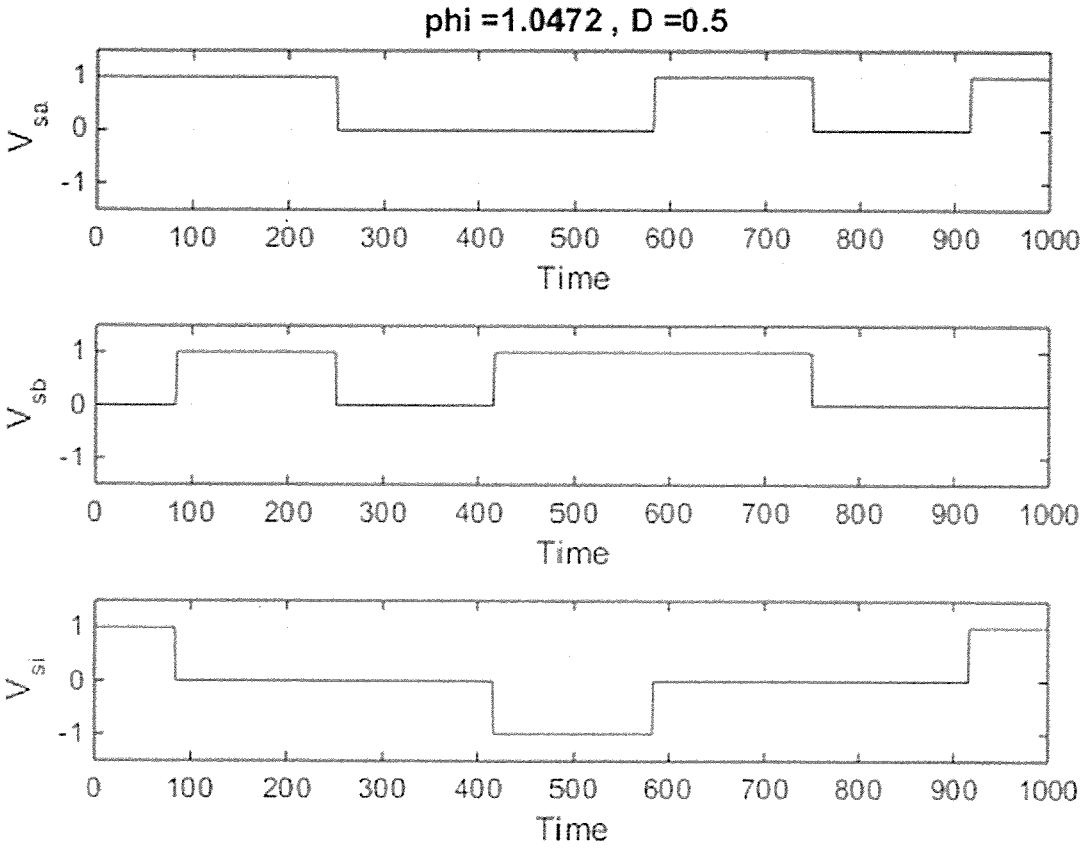

phi =1.0472 , D =0.5
V_{sa}
V_{sb}
V_{si}
1
0
-1
0
100
200
300
400
500
600
700
800
900
1000
Time

FIG.5E

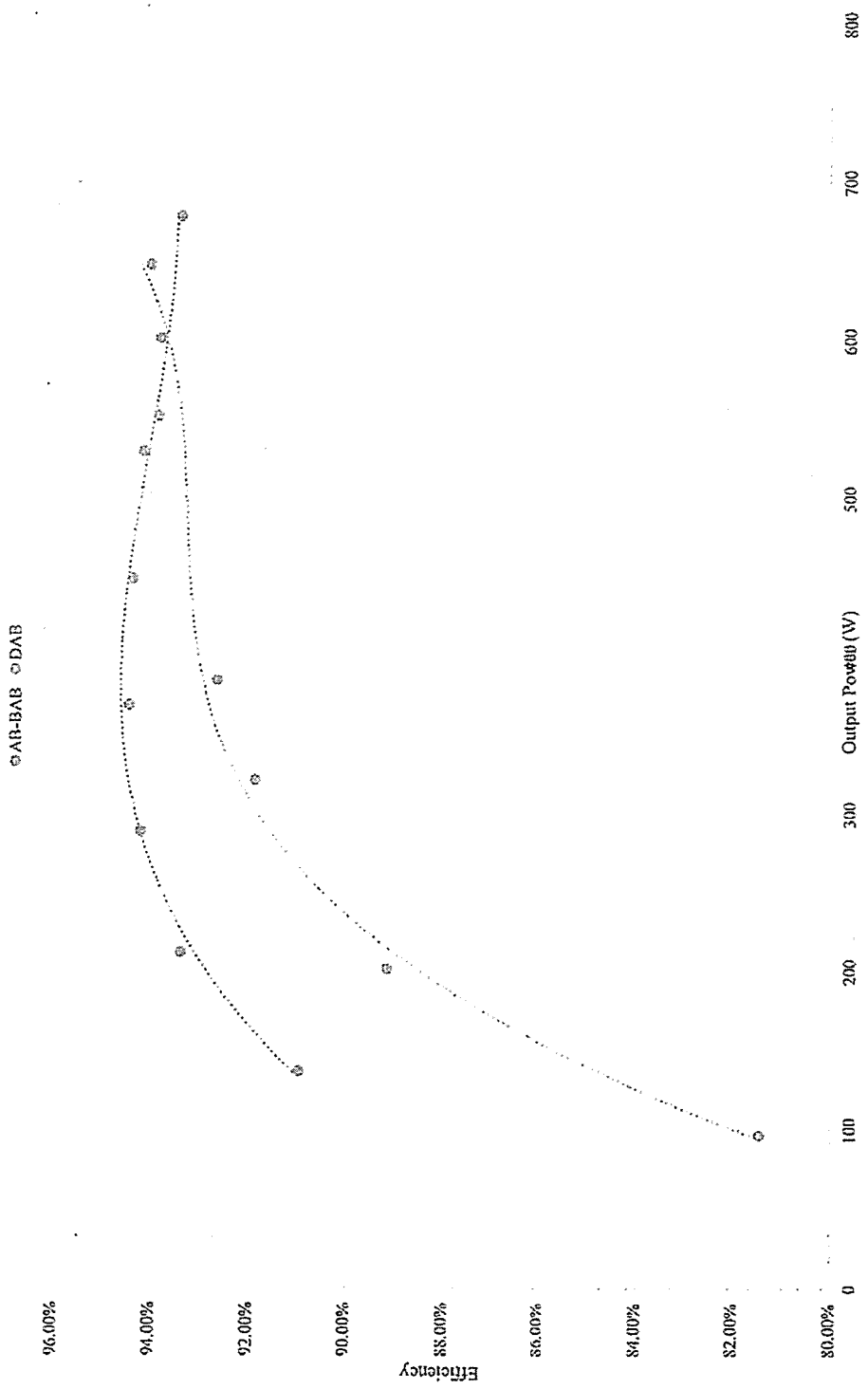

AR-BAB
DAB
Output Power (W)
0
100
200
300
500
600
700
800
Efficiency
80.00%
82.00%
84.00%
86.00%
88.00%
90.00%
92.00%
94.00%
96.00%

FIG.6

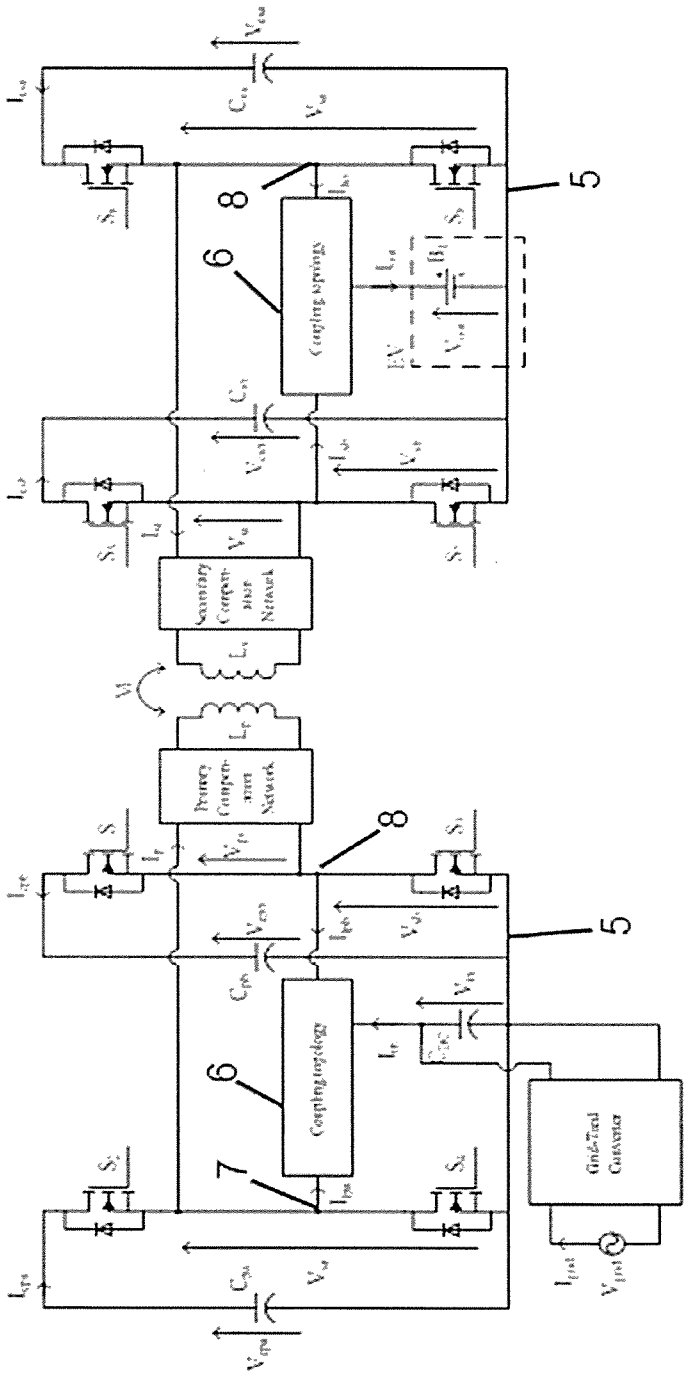

5
8
6
7
Coupling Inductor
Primary Compensation Network
Secondary Compensation Network
Grid/Load Converter

FIG.7

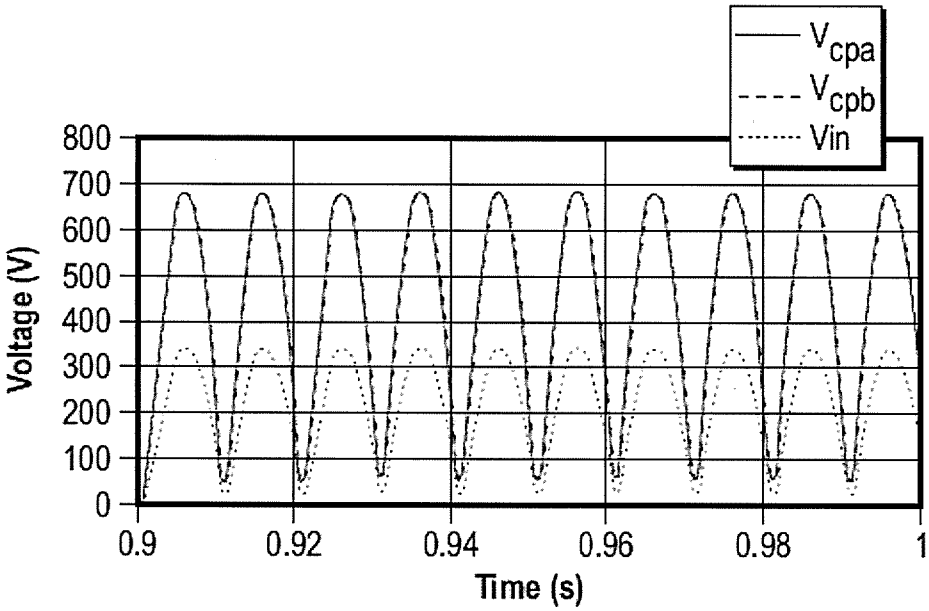

V_{cpa}
V_{cpb}
Vin
800
700
600
500
400
300
200
100
0
Voltage (V)
0.9
0.92
0.94
0.96
0.98
1
Time (s)

FIG. 8A

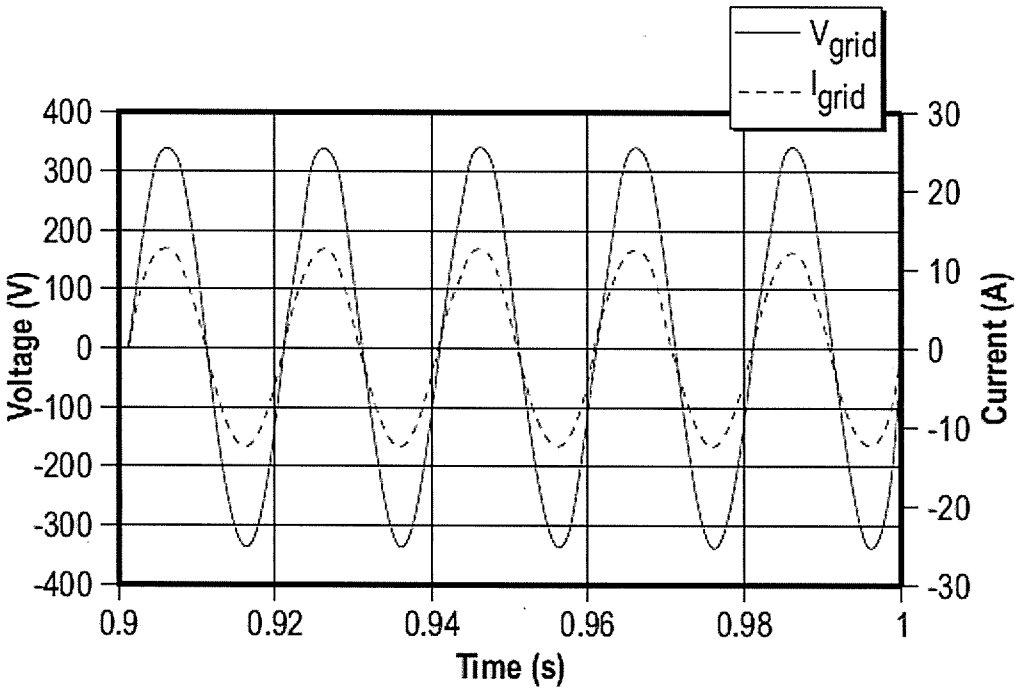

V_{grid}
I_{grid}
400
300
200
100
0
-100
-200
-300
-400
Voltage (V)
30
20
10
0
-10
-20
-30
Current (A)
0.9
0.92
0.94
0.96
0.98
1
Time (s)

FIG. 8B

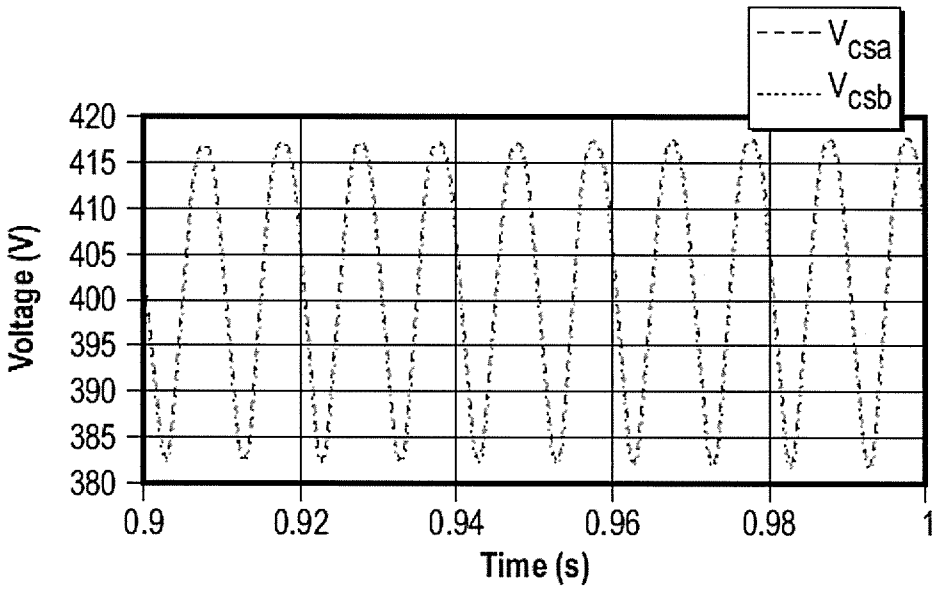

Vcsa
Vcsb
420
415
410
405
400
395
390
385
380
Voltage (V)
0.9
0.92
0.94
0.96
0.98
1
Time (s)

FIG. 8C

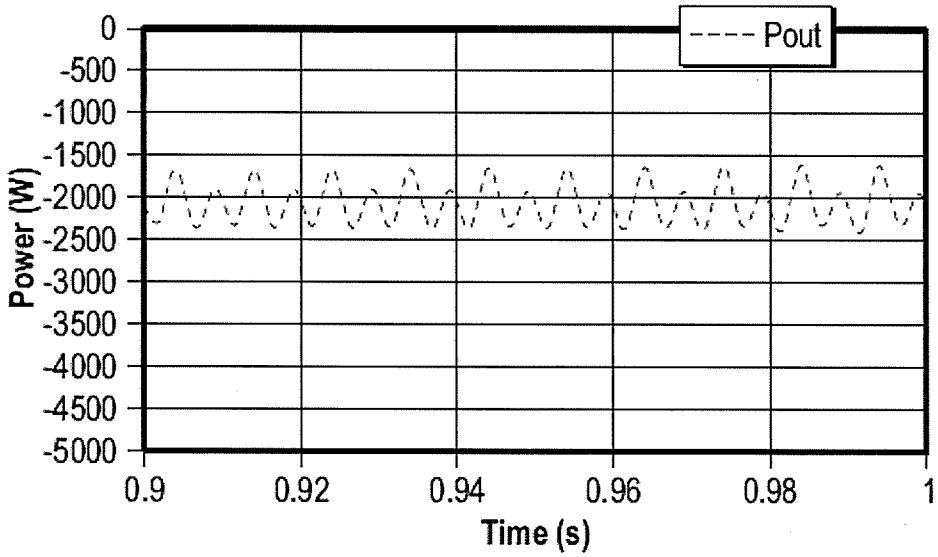

Pout
0
-500
-1000
-1500
-2000
-2500
-3000
-3500
-4000
-4500
-5000
Power (W)
0.9
0.92
0.94
0.96
0.98
1
Time (s)

FIG. 8D

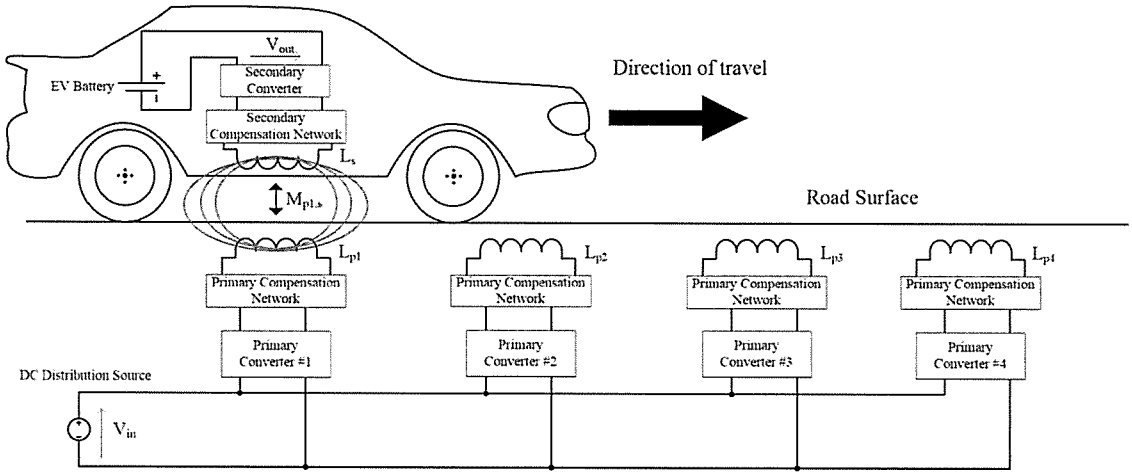

V_{out}
EV Battery
Secondary Converter
Secondary Compensation Network
L_s
$M_{p1,s}$
Direction of travel
Road Surface
L_{p1}
L_{p2}
L_{p3}
L_{p4}
Primary Compensation Network
Primary Compensation Network
Primary Compensation Network
Primary Compensation Network
Primary Converter #1
Primary Converter #2
Primary Converter #3
Primary Converter #4
DC Distribution Source
V_{in}

FIG.9

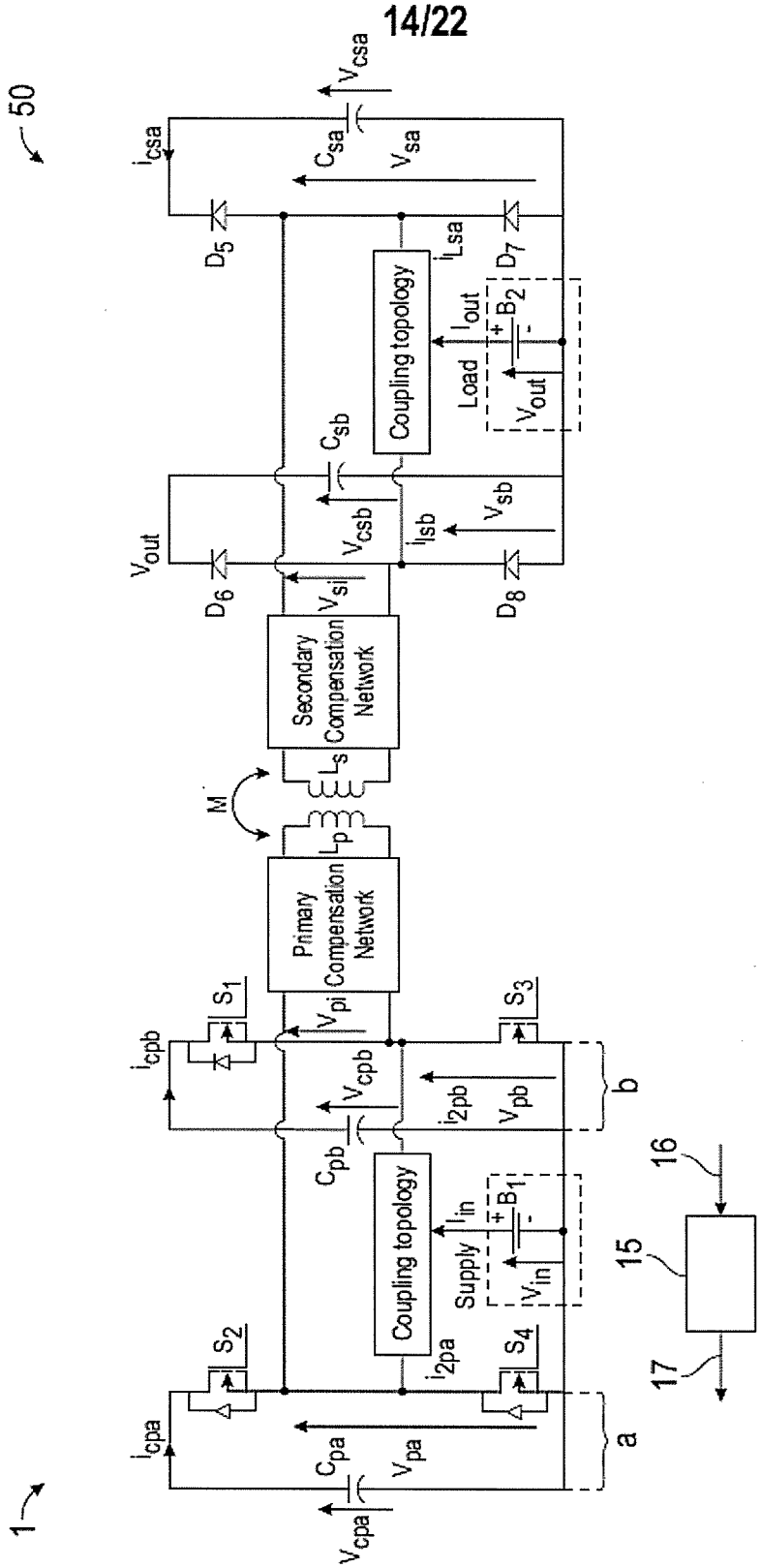

50
1
V_{csa}
C_{sa}
V_{sa}
i_{csa}
D_5
D_7
i_{Lsa}
Coupling topology
i_{out}
B_2
Load
V_{out}
C_{sb}
V_{csb}
i_{Lsb}
V_{sb}
V_{out}
D_6
D_8
V_{si}
Secondary Compensation Network
L_s
M
L_p
Primary Compensation Network
V_{pi}
S_1
S_3
i_{cpb}
V_{cpb}
i_{2pb}
V_{pb}
b
C_{pb}
Coupling topology
i_{in}
B_1
Supply
V_{in}
16
15
17
S_2
S_4
i_{2pa}
i_{cpa}
C_{pa}
V_{pa}
a
V_{cpa}

FIG. 10

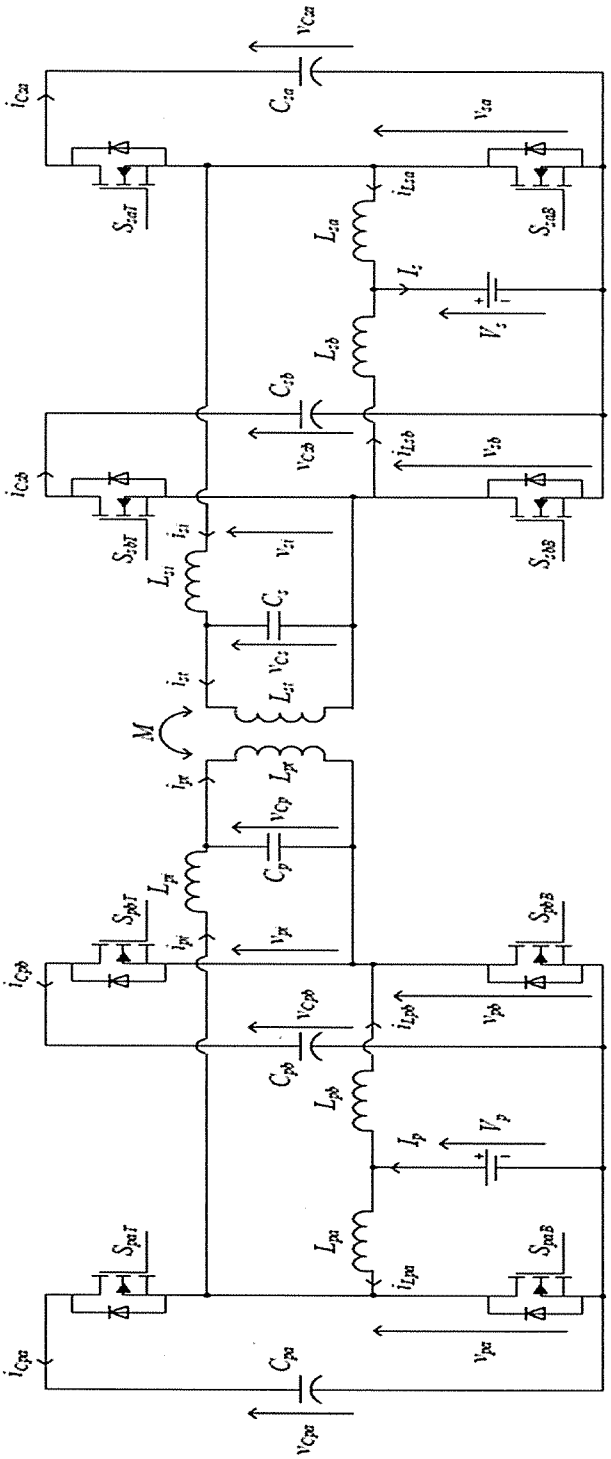


FIG.11

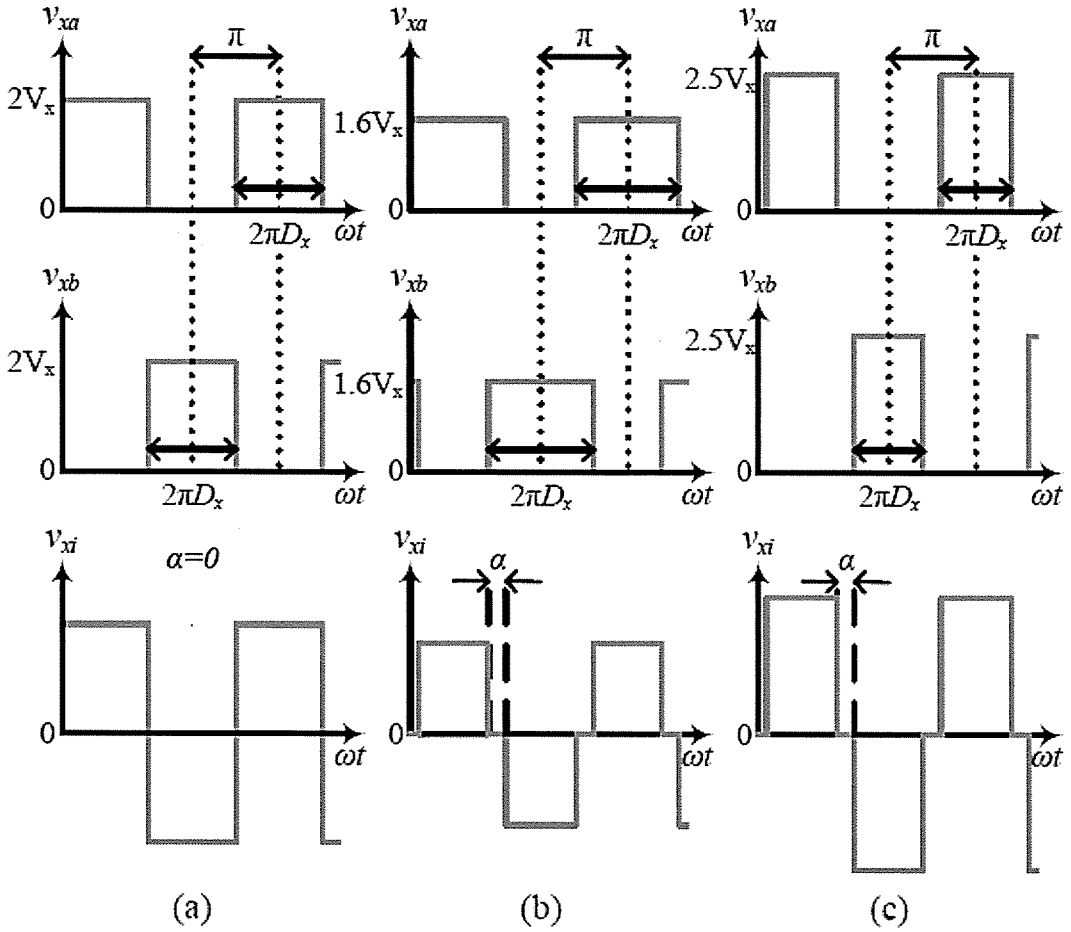

v_{xa}
v_{xb}
v_{xi}
π
$2V_x$
$1.6V_x$
$2.5V_x$
0
$2\pi D_x$
ωt
α=0
α
(a)
(b)
(c)

FIG.12

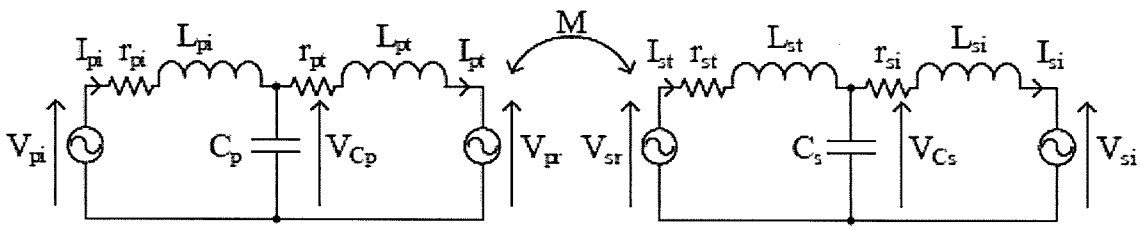

I_{pi} r_{pi} L_{pi} r_{pt} L_{pt} I_{pt}
M
I_{st} r_{st} L_{st} r_{si} L_{si} I_{si}
V_{pi}
C_p
V_{Cp}
V_{pr}
V_{sr}
C_s
V_{Cs}
V_{si}

FIG.13

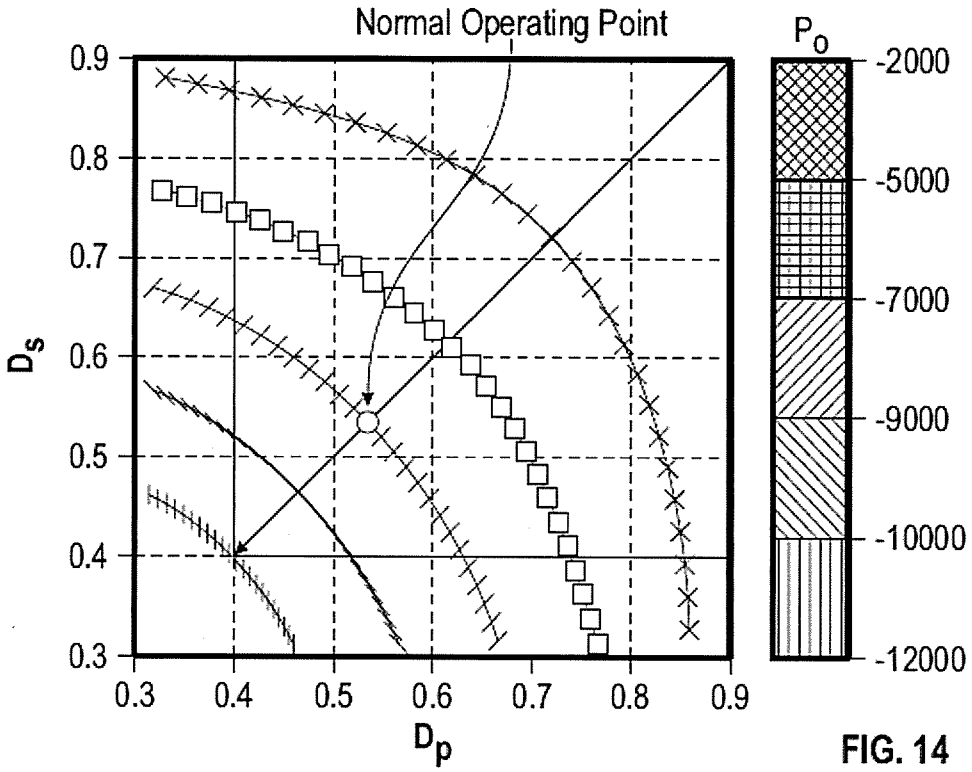

Normal Operating Point
P_o
-2000
-5000
-7000
-9000
-10000
-12000
0.9
0.8
0.7
0.6
0.5
0.4
0.3
D_s
0.3 0.4 0.5 0.6 0.7 0.8 0.9
D_p

FIG. 14

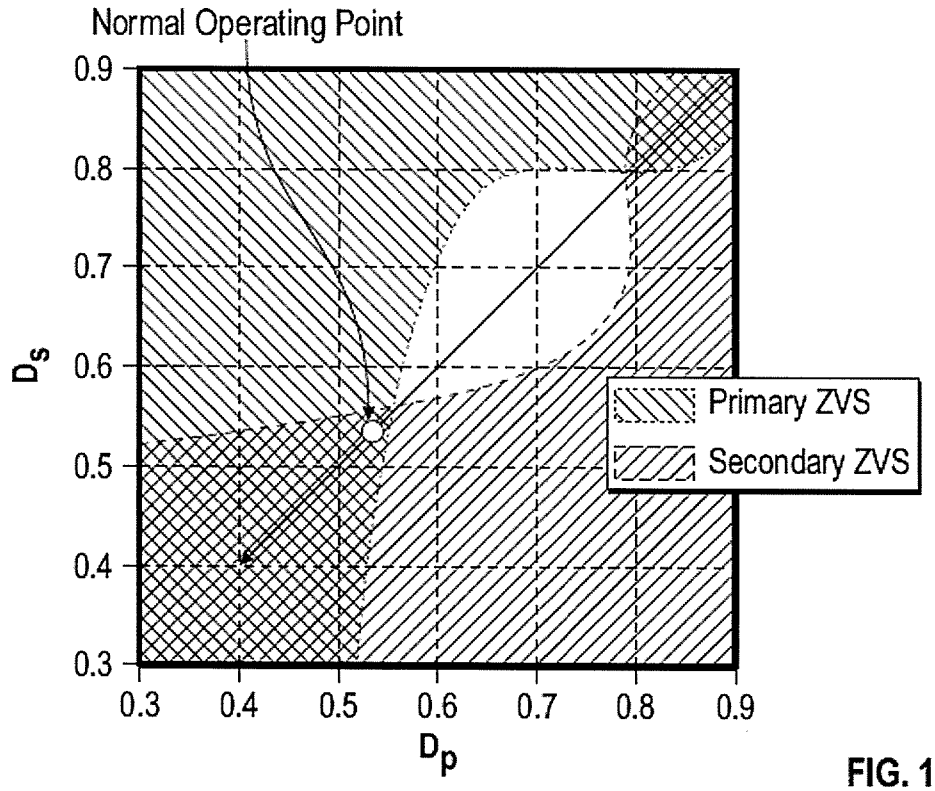

Normal Operating Point
0.9
0.8
0.7
0.6
0.5
0.4
0.3
D_s
0.3 0.4 0.5 0.6 0.7 0.8 0.9
D_p
Primary ZVS
Secondary ZVS

FIG. 15

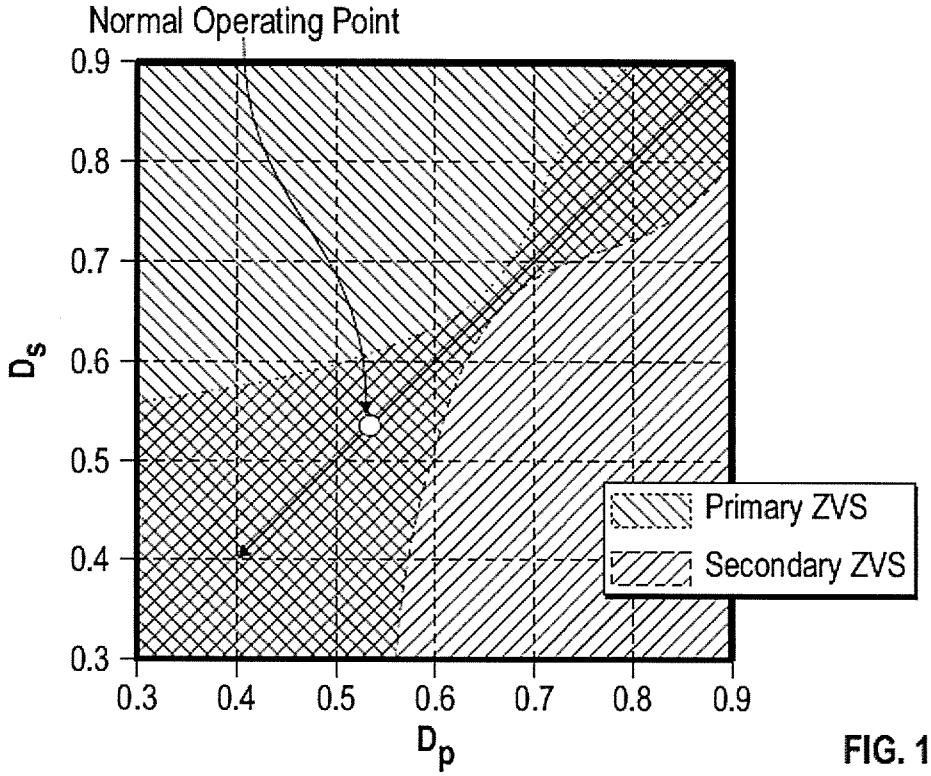

Normal Operating Point
0.9
0.8
0.7
0.6
0.5
0.4
0.3
D_s
0.3 0.4 0.5 0.6 0.7 0.8 0.9
D_p
Primary ZVS
Secondary ZVS

FIG. 16

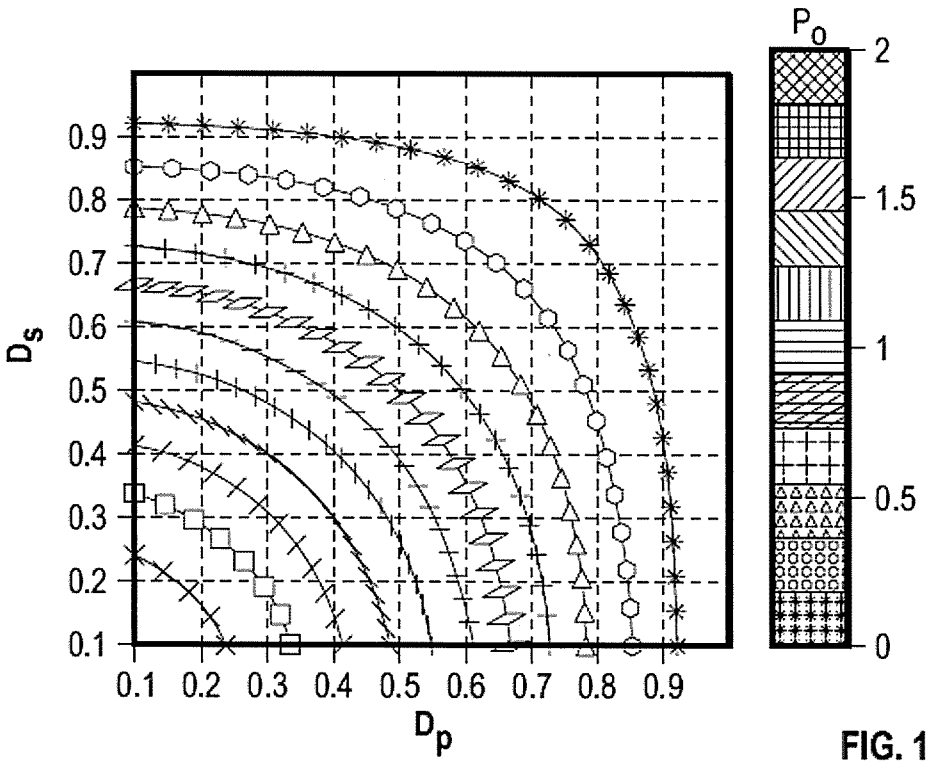

P_o
2
1.5
1
0.5
0
0.9
0.8
0.7
0.6
0.5
0.4
0.3
0.2
0.1
D_s
0.1 0.2 0.3 0.4 0.5 0.6 0.7 0.8 0.9
D_p

FIG. 17

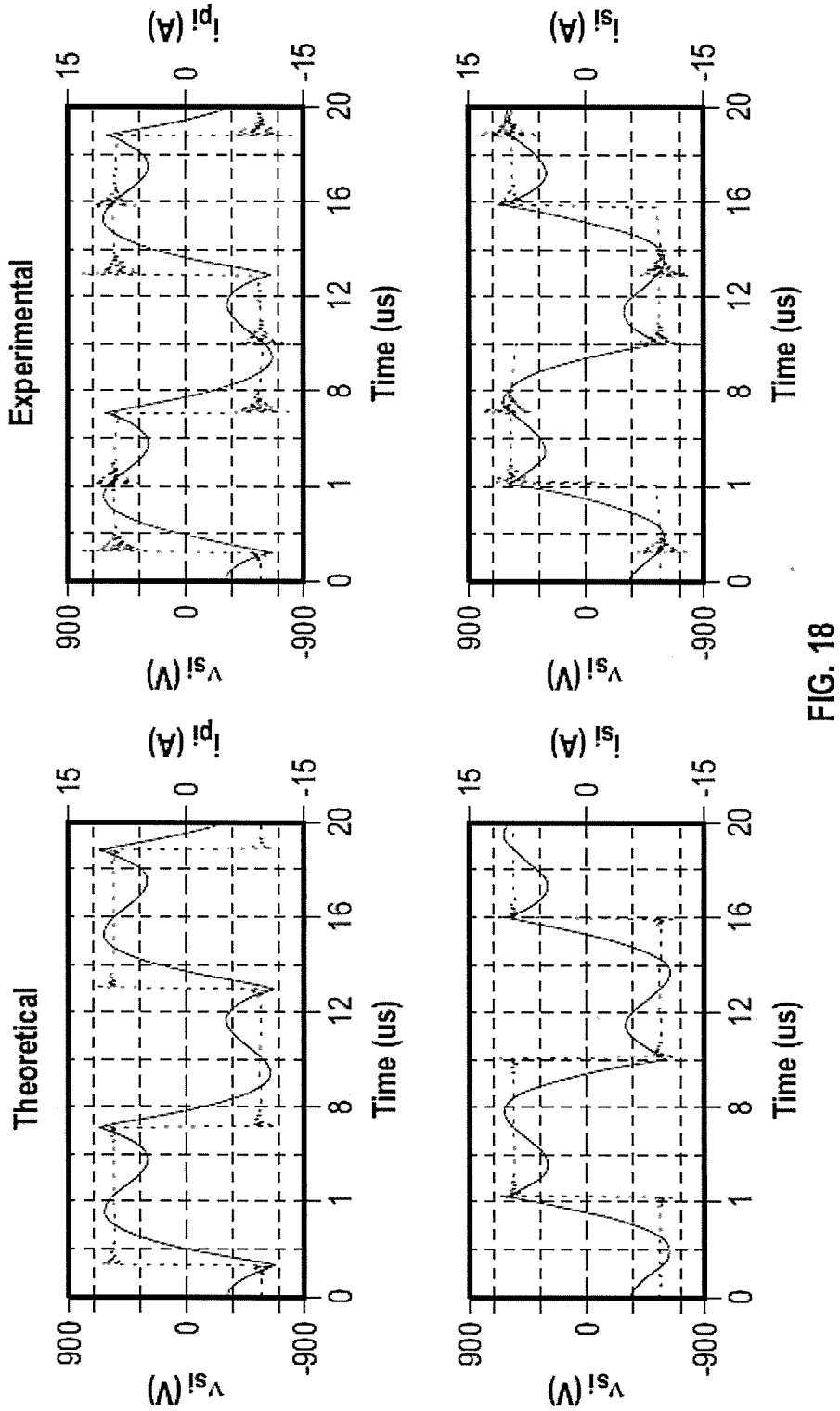

Experimental
Theoretical
i_{pi} (A)
i_{si} (A)
v_{si} (V)
Time (us)
15
0
-15
900
-900
0
1
8
12
16
20

FIG. 18

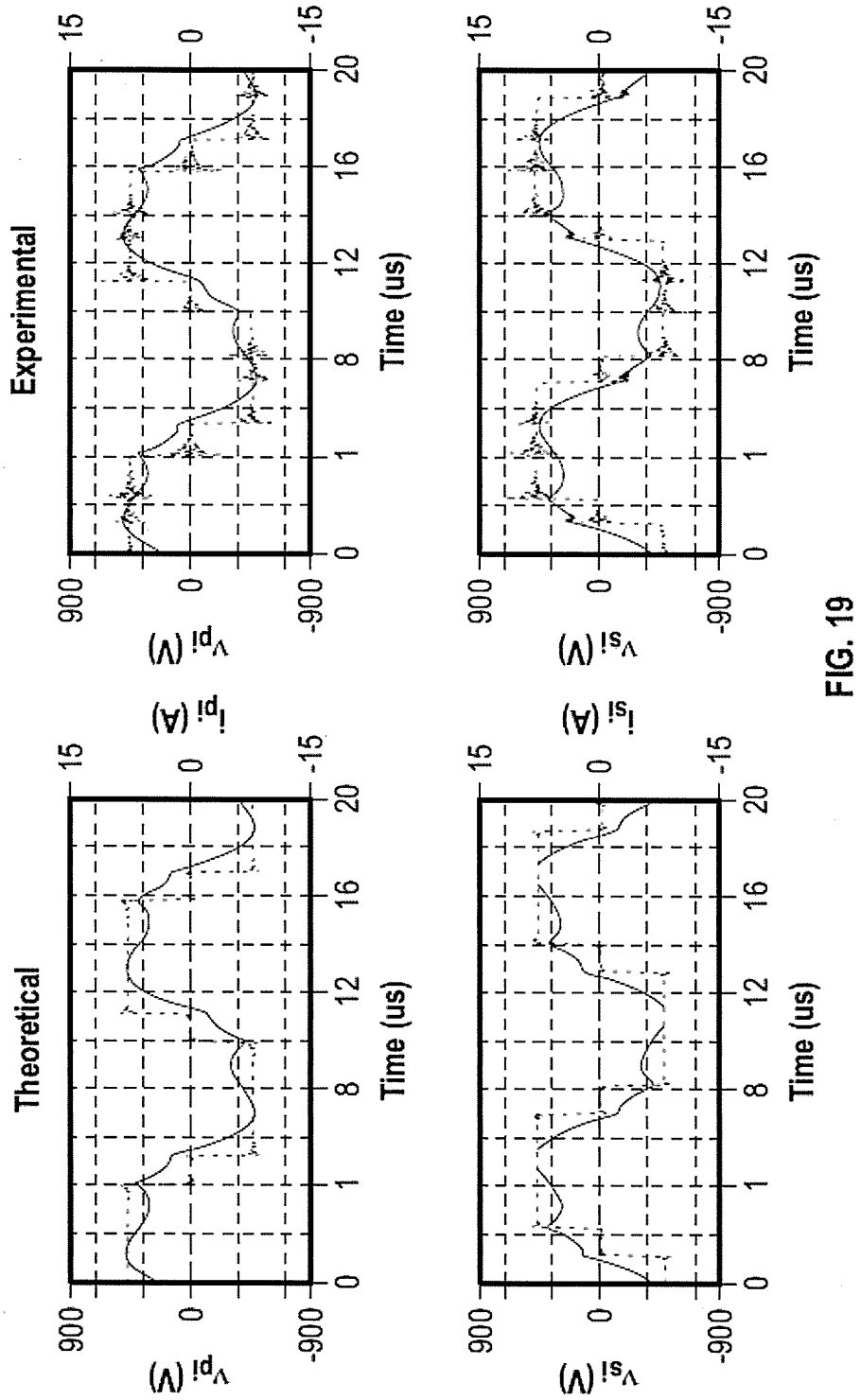

Experimental
Theoretical
Time (us)
Time (us)
Time (us)
Time (us)
v_{pi} (V)
i_{pi} (A)
v_{si} (V)
i_{si} (A)
900
0
-900
15
0
-15
0
1
8
12
16
20

FIG. 19

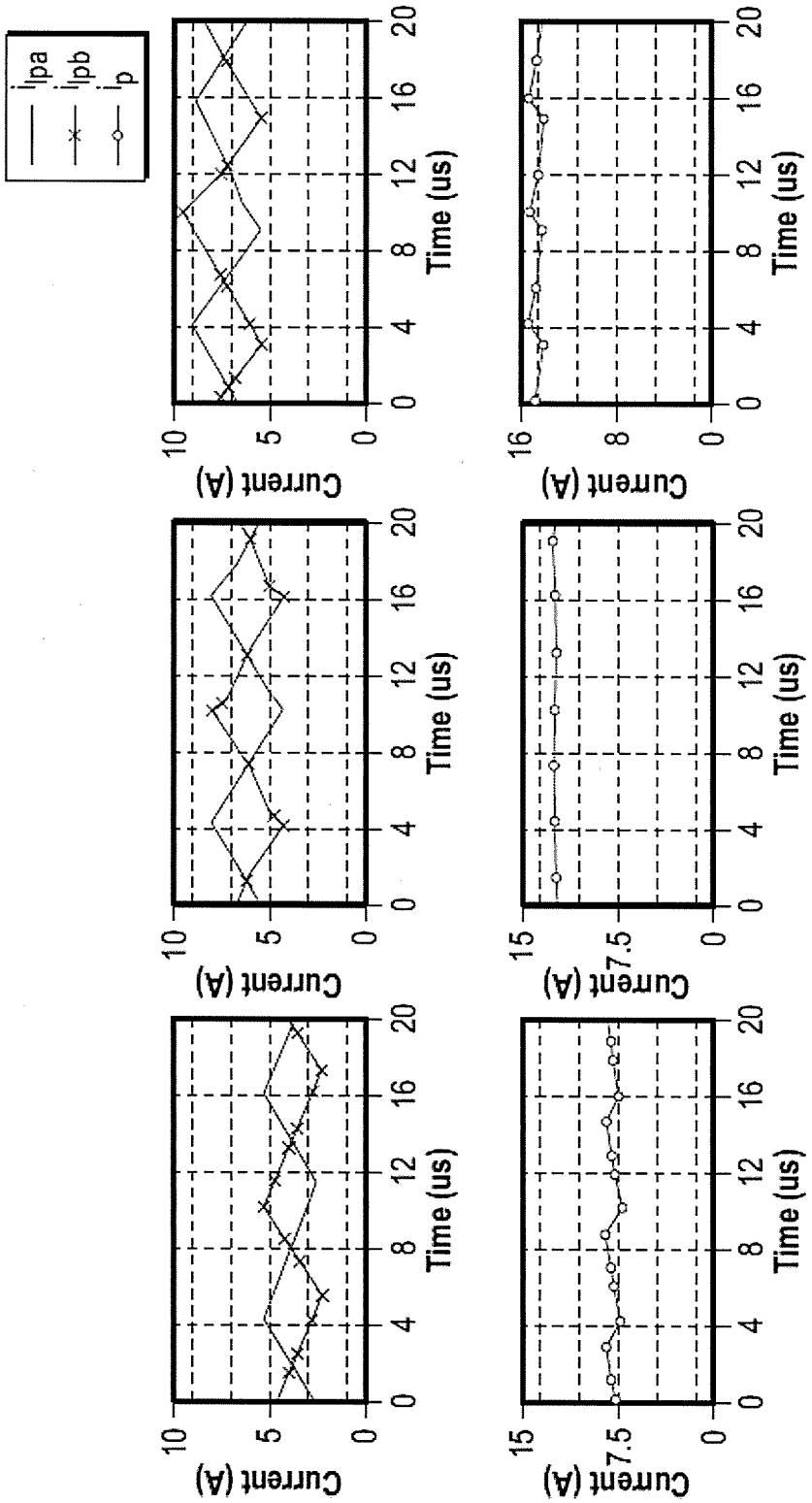


FIG. 20

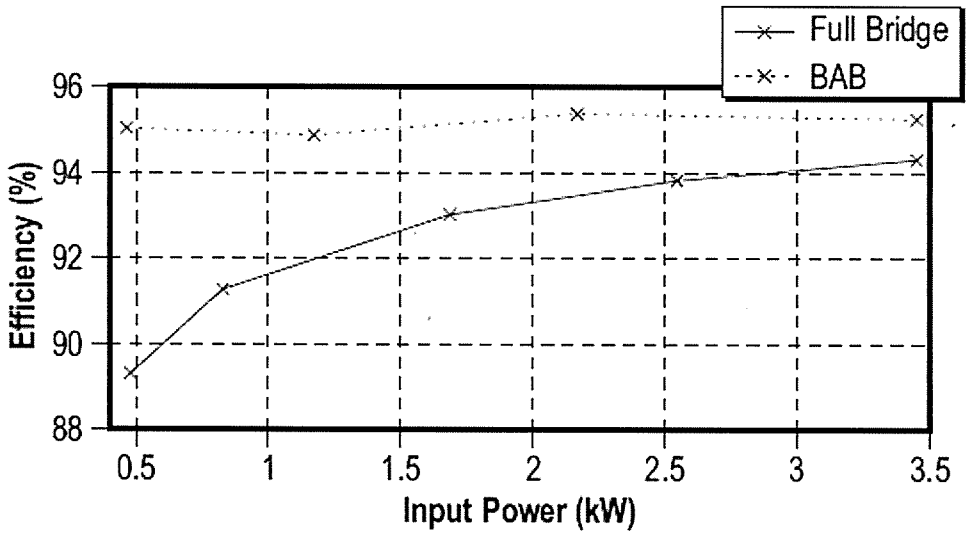

Full Bridge
BAB
96
94
92
90
88
Efficiency (%)
0.5
1
1.5
2
2.5
3
3.5
Input Power (kW)

FIG. 21

INTERNATIONAL SEARCH REPORT

International application No.
PCT/NZ2018/050039

A. CLASSIFICATION OF SUBJECT MATTER

H02J 50/00 (2016.01) H02M 5/04 (2006.01) H04B 5/00 (2006.01)

According to International Patent Classification (IPC) or to both national classification and IPC

B. FIELDS SEARCHED

Minimum documentation searched (classification system followed by classification symbols)

Documentation searched other than minimum documentation to the extent that such documents are included in the fields searched

Electronic data base consulted during the international search (name of data base and, where practicable, search terms used)

PATENW (WPIAP, EPODOC, TXTE) IPC/CPC: H02J50/00, H02M5/00, H04B5/00; keywords: AC TO AC CONVERTER, BRIDGE, SECOND ENERGY SOURCE, ACTIVE BRIDGE, BI-DIRECTIONAL and similar terms and phrases.

GOOGLE keywords: AC TO AC CONVERTER, IPT, SUPPLEMENTARY POWER SUPPLY, SECOND ENERGY SOURCE, ACTIVE BRIDGE and similar terms and phrases.

Applicant(s)/Inventor(s) names searched in Esp@cenet, Auspat and internal databases provided by IP Australia.

C. DOCUMENTS CONSIDERED TO BE RELEVANT

Category*	Citation of document, with indication, where appropriate, of the relevant passages	Relevant to claim No.
	Documents are listed in the continuation of Box C	

[X] Further documents are listed in the continuation of Box C [X] See patent family annex

* Special categories of cited documents:

"A" document defining the general state of the art which is not considered to be of particular relevance

"E" earlier application or patent but published on or after the international filing date

"L" document which may throw doubts on priority claim(s) or which is cited to establish the publication date of another citation or other special reason (as specified)

"O" document referring to an oral disclosure, use, exhibition or other means

"P" document published prior to the international filing date but later than the priority date claimed

"T" later document published after the international filing date or priority date and not in conflict with the application but cited to understand the principle or theory underlying the invention

"X" document of particular relevance; the claimed invention cannot be considered novel or cannot be considered to involve an inventive step when the document is taken alone

"Y" document of particular relevance; the claimed invention cannot be considered to involve an inventive step when the document is combined with one or more other such documents, such combination being obvious to a person skilled in the art

"&" document member of the same patent family

Date of the actual completion of the international search	Date of mailing of the international search report
1 August 2018	01 August 2018

Name and mailing address of the ISA/AU

AUSTRALIAN PATENT OFFICE
PO BOX 200, WODEN ACT 2606, AUSTRALIA
Email address: pct@ipaustralia.gov.au

Authorised officer

Bayer Mitrovic
AUSTRALIAN PATENT OFFICE
(ISO 9001 Quality Certified Service)
Telephone No. +61262832164

INTERNATIONAL SEARCH REPORT		International application No.
C (Continuation).	DOCUMENTS CONSIDERED TO BE RELEVANT	**PCT/NZ2018/050039**

Category*	Citation of document, with indication, where appropriate, of the relevant passages	Relevant to claim No.
X	DUTTA SUMIT:" Controls and Applications of the Dual Active Bridge DC to DC Converter for Solid State Transformer Applications and Integration of Multiple Renewable Energy Sources", PhD thesis, Department of Electrical Engineering, North Carolina State University, USA, 2014, p.1-201. Available on the Internet at: https://repository.lib.ncsu.edu/handle/1840.16/9710, Downloaded on 20.07.2018. Whole document, especially abstract, Chapters 2 and 3, especially Figs. 3.4- 3.10 and 3.44	1-22
X	WALBERMARK M.DOS SANTOS ET AL.:"DC microgrids with photovoltaic generation and high frequency isolation connected to utility grid",2013 Brazilian Power Electronics Conference, IEEE, 2013, p.636-641. Whole document, especially abstract, Fig.1.	1-22
A	HENGSI QIN ET AL.:"AC-AC dual active bridge converter for solid state transformer", 2009 IEEE Energy Conversion Congress and Exposition, IEEE 2009, p.3039-3044. Whole document.	1-22

INTERNATIONAL SEARCH REPORT Information on patent family members	International application No. **PCT/NZ2018/050039**

This Annex lists known patent family members relating to the patent documents cited in the above-mentioned international search report. The Australian Patent Office is in no way liable for these particulars which are merely given for the purpose of information.

Patent Document/s Cited in Search Report		**Patent Family Member/s**	
Publication Number	**Publication Date**	**Publication Number**	**Publication Date**

End of Annex

Due to data integration issues this family listing may not include 10 digit Australian applications filed since May 2001.